ABSTRACT

JUNG, UI KYUNG. Digital Textile Printing with Laser Engraving: Surface Contour Modification and Color Properties (Under the direction of Dr. Traci May Lamar).

This research combines two digital technologies for customizing textile substrates: carbon dioxide (CO_2) laser treatment and digital textile printing. They are highly versatile surface design technologies that provide great detail, enhance design flexibility, and meet the growing consumer demand for novelty and variety in apparel and textile designs. One of the most important aesthetic effects of combining those technologies is the potential to influence the color properties of digitally printed textile materials by laser treating the material surface before printing. The objective of this research is to determine if creating pile height variation by laser engraving cotton velvet fabric prior to digital inkjet printing can impact the resulting color. Because color yield depends on the surface in contact with the dye, a pile fabric (cotton velvet) was selected for this investigation.

To develop samples, laser engraving was conducted to create pile height variance before printing using a 60W CO_2 laser machine. The laser settings were held constant with 100% speed, 70% power and 400 dots per inch resolution. Laser intensity was controlled by using 0%, 25%, 50%, 75%, and 100% grayscale patterns to modify pile height and surface contour of velvet. Higher intensities remove more of the surface pile. After laser treatment, seven solid cyan, magenta, yellow, black, red, green, and blue colored stripes were printed with a reactive dye ink printer.

After sample development, the color properties of the fabrics were measured by using a spectrophotometer with D_{65} daylight and 10° standard observer. Reflectance curves, CIE L*a*b*, C*, ΔE_{cmc}, K/S_{sum} values were obtained and interpreted to compare color consistency depending on pile height variation. According to the results, pile height variation was demonstrated to cause a measurable effect on color results in inkjet printing using instrumental measures.

Digital Textile Printing with Laser Engraving: Surface Contour Modification and Color Properties.

by
Ui Kyung Jung

A thesis submitted to the Graduate Faculty of
North Carolina State University
in partial fulfillment of the
requirements for the degree of
Master of Science

Textiles

Raleigh, North Carolina

2019

APPROVED BY:

_____	_____
Dr. Traci A.M. Lamar Committee Chair	Dr. Renzo Shamey
_____	
Dr. Lisa Chapman	

DEDICATION

To my parents, my brother Minjoon Jung, and my husband Wonkyung Jang.

BIOGRAPHY

Uikyung Jung received her Bachelor of Science in Clothing and Textiles and Business Administration from Ewha Womans University in 2016. She began her Master's degree program in Textiles in the Wilson College of Textiles at North Carolina State University in Fall 2017 and decided to proceed with her study to the Ph.D. program from Fall 2019.

ACKNOWLEDGMENTS

I would like to first acknowledge my adviser Dr. Traci Lamar for her support, guidance, and advice. I also would like to thank Dr. Renzo Shamey, without whom my research was not feasible. I further would like to thank Dr. Lisa Chapman for her help and support issues regarding digital inkjet printing.

Special thanks to Jeff Krauss, Tri Vu, Bailey Knight, Ming Wang, Jiajun Liu, Yixin Liu, and Nian Xiong for their time and consideration to help me with pretreatment, printing, posttreatment, and color measurement.

TABLE OF CONTENTS

LIST OF TABLES

LIST OF FIGURES

CHAPTER 1: INTRODUCTION

This research combines two digital technologies for customizing textile substrates: carbon dioxide CO2 laser treatment and digital textile printing. With laser treatment and digital printing technology, various textures and patterns can be created on fabrics. One of the most important aesthetic effects of applying these technologies is the modification of the color properties of the textile materials. The objective of this research was to assess the color quality of inkjet-printed colors on cotton velvet fabric with pile height variance created by treatment with different laser intensities. Because color yield depends on the surface in contact with the dye (Kan et al., 2011), it was anticipated that variation in the pile height of a pile fabric would influence colorimetric attributes of the substrate.

1.1 Research Objective and Questions

The research objective is to determine if creating pile height variation by laser engraving cotton velvet fabric prior to digital inkjet printing can impact the resulting color. There are two research questions:

[1] Does the pile height variance created by treating fabrics at differing laser intensities result in instrumentally measurable differences in fabric's color properties?

[2] Does the pile height variance created by treating at differing laser intensities result in instrumentally measurable differences in color properties based on printed color?

1.2 Significance of Research

Color is one of the most important factors affecting the quality of fabric (Endo et al., 2013). However, the color of the fabric is influenced by its texture (Endo et al., 2013; Kandi et al., 2008; Kitaguchi et al., 2005; Shao et al., 2006; Xin et al., 2005). The precedent studies focused on inkjet printing quality and color attributes on woven, knitted and nonwoven fabric constructions and their

surface characteristics (Bae, et al., 2015; Carr, et al., 2006; Choudhury, 2014b; Janssen, 2017; Luo, et al., 2015; Mhetre, et al., 2010; Park, et al., 2006). Furthermore, many studies focused on ink formulation and pretreatment which can affect the quality of printed fabric (Abd El-Wahab, et al., 2010; Daplyn & Lin, 2003; Ding, et al., 2019; Fan, et al., 2002; Lim & Chapman, 2019; Liu, et al., 2016). However, limited studies have concentrated on inkjet printing on pile fabric. In this research, the influence of the textured surface of a pile fabric on its instrumental color measurements will be investigated.

Pile fabrics are distinguished from other textiles by their surface, where an almost infinite number of fibers stand erect from the foundation structure of the cloth (Gladstone, 1970). Pile surfaces are suitable for sculpture with lasers through partial and controlled removal of portions of fibers and creating variations in fiber height. In addition, in digital inkjet printing most of the ink reacts with the surface of the fibers instead of penetrating the core, thus fabric surface topology and structure can affect the amount of ink that reacts with the fiber and hence its resulting colorimetric properties (Bae et al., 2015; Lim & Chapman, 2019). Researchers have previously indicated the possibility of creating certain design effects by controlling the intensity of the laser and removing the colorant present on the surface of the fabric and by altering the coloration properties and the dyeability of substrates (Bahtiyari, 2011; Kan, 2014; Shahidi et al., 2013).

Furthermore, this study will fundamentally demonstrate the effectiveness of combining digital textile printing and laser treatment for creating multiple variations in texture and color on a given substrate. In today's fashion world, technology has taken on an important role in the creation of novel design effects. As types of digital technology, these two technologies are applied for decorative, and coloration purposes with unique fashion design looks. With these technologies, simple and complex patterns can be created on the surface of garments. Since both technologies

are used in conjunction with computer-aided design, creating a digital file to submit to a computer cuts down on cost and time, making this process is highly accurate and repeatable. Customization systems are valuable tools for addressing sustainability and consumer demands.

CHAPTER 2: LITERATURE REVIEW

2.1 Pile Fabric: Velvet

2.1.1 Introduction to Velvet Fabric

When compared to other textiles, pile fabrics such as velvet, terry cloth, chenille, and pile carpets, have differences which can be seen in their surface that has unlimited tufts or loops of fibers or yarns that stand straight from the foundation structure of the cloth (Gong, 2015). The main quality determinants for all pile fabrics are the density and evenness of the fibers on the surface and the pile height, respectively, the luster of the finish, and a general rich look on the surface (Gladstone, 1970).

The existence of velvet fabrics can be traced back to as early as 2000 BC (Brandon, 2008) and the processes including tufting, knitting, knotting, flocking, and nonwovens are used to make them (Gong, 2015). The cut pile woven fabric is the most common type of velvet that finds wide use in apparel and products used for furnishing homes. Its production involves extra warp yarns that are used during weaving in between the layers of the cloth or on the surface of the fabric, and cutting of yarns to the required height (Redmore, 2011).

Figure 2.1 The Cross-Section of Velvet Fabric ("Fancy Weaves", n.d.)

2.1.2 The production of velvet

An extra set of warp yarns are used to produce loops at regular intervals for the production of velvets; a cutting blade is withdrawn to cut the loop (Redmore, 2011). A tight plain weave is formed by the ground warp that holds the pile yarns in their place. A double cloth or a two-layer

construction is another popular way to produce velvet, which involves two cloths woven together, face-to-face (Redmore, 2011). The pile yarn weaves up and down between the two layers of ground fabric in this process. Then this interlinkage, while it is still on the loom, is cut through the middle creating two velvet fabrics (Figure 2.2).

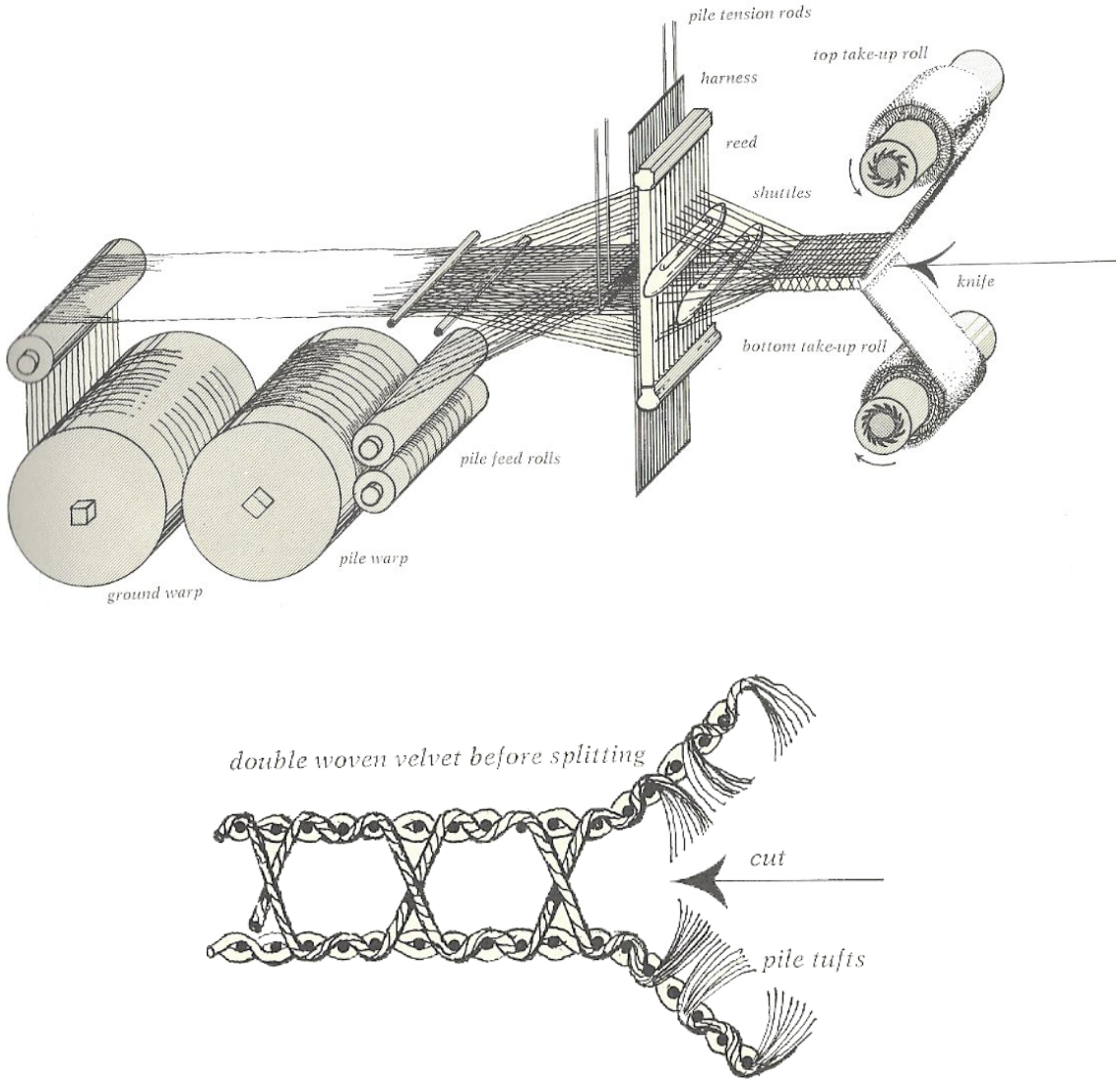

Figure 2.2 Production of Velvet (Gladstone, 1970)

2.2 Laser Technology

2.2.1 Introduction to laser technologies

A laser can be used to cut different types of objects that range from stretchable fabric to hard metal (Belli et al. 2005; Ondogan et al. 2005; Vilumsone-Nemes, 2018). A concentrated laser beam when directed at a material, either melts, burns, or vaporizes it and leaves a high-quality finished edge (Bogue, 2015). Lasers can also be utilized in various ways through cutting, perforating, drilling, engraving, marking, creasing, structuring, and welding (Vilumsone-Nemes, I., 2018).

The use of laser tools has seen an increase in popularity in industries dealing with textiles, leather, and garments as they are useful for achieving greater efficiency while reducing costs. Costs are reduced by removing the handling systems in comparison to the regular tools for cutting like band blades, discs, and reciprocating knives (Nayak & Padhye, 2016).

A collimated beam used in laser cutting operations can be concentrated into a very fine dot of intense energy for precise cutting. The same laser source is capable of performing various laser treatments on textiles by controlling laser power scrupulously (Nayak & Padhye, 2016; Vilumsone-Nemes, 2018). The potential to damage the product in cutting is diminished as the cutting tool and the material do not physically contact. A laser is also capable of cutting very fragile materials and parts with little or no support (Vilumsone-Nemes, 2018). Last but not least, the laser technique does not pollute or waste any material and there is no need for disposing of any toxic by-product (Nayak & Padhye, 2016).

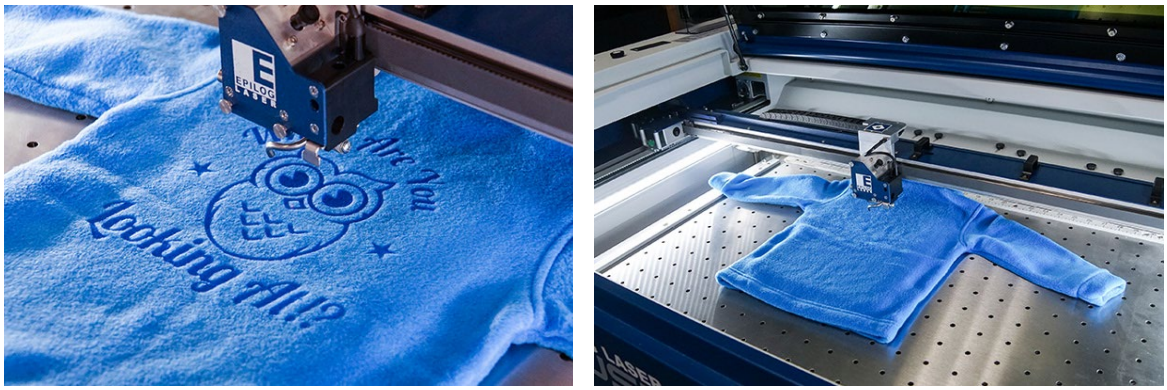

Figure 2.3 Laser Engraved Fleece Jacket ("How to Laser Engrave a Child's Fleece Jacket," n.d.)

2.2.2 Principle of CO_2 Laser Machine

A laser system includes a laser source, a cutting head, an optical system, software to regulate the laser, a cutting table, and a system of the extraction that removes the smoke particles formed in the process of laser cutting. The cutting process involves focusing and intensifying the light from a laser source using a lens or mirror that creates a laser beam at the cut surface (Vilumsone-Nemes, 2018).

A laser beam is produced in an enclosed tube by stimulating a lasing material with electric emission that is high in frequency (Figure 2.4). Part of the emitted energy is sent out as laser radiation by a gas, which acts as a laser-active medium. To produce the CO_2 laser beam, a gas of three combined elements in a sealed discharge tube is utilized: the three components are, carbon dioxide (CO_2), nitrogen (N_2), and helium (He), which are present in the ratio of 1:2:3 (Vilumsone-Nemes, 2018).

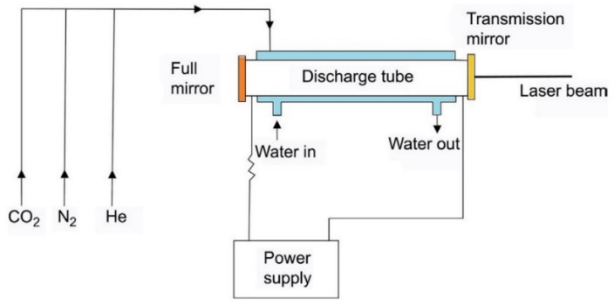

Figure 2.4 Schema of Elements Producing a Laser Beam (Vilumsone-Nemes, 2018)

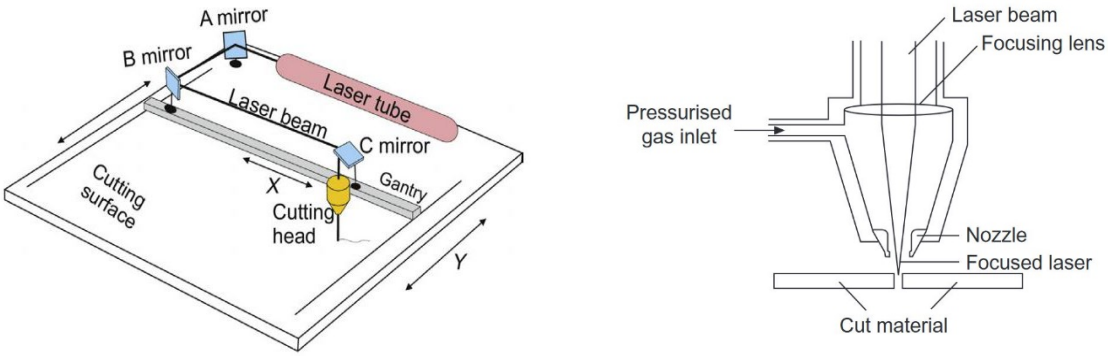

Figure 2.5 (Left) System of Laser Beam Guidance in a Flatbed Laser Cutter, and (Right) Laser Cutting Head (Vilumsone-Nemes, 2018)

If the energy of the atoms and molecules of the gas is excited to sufficient intensity, the gas mixture can generate a laser. Through mirrors present at both ends of the discharge tube, the light energy is reflected back and forth many times (Figure 2.5). To get the optimal coherence and power outcome, and to reflect the laser to the working zone, many partial mirrors are used inducing multiple internal reflections in the laser tube (Nayak & Padhye, 2016).

When a laser light beam is concentrated on the surface of the fabric, it increases the temperature considerably, and melts, burns, and vaporizes the material. According to the level of

applied laser power, the cutting, perforation, marking, engraving, and heat sealing of the textile materials can happen (Nayak & Padhye, 2016; Vilumsone-Nemes, 2018).

2.2.3 Process of conducting CO_2 laser treatment

The process of laser cutting or engraving on fabric begins by exploiting the Adobe Illustrator software to produce a graphic and then sending the graphic file to the laser system. Next the parameters of laser power, speed, and pixels per inch are set. After this, the fabric is loaded and positioned on the cutting table. In the final step, the laser is directed onto the fabric (Yuan et al., 2012).

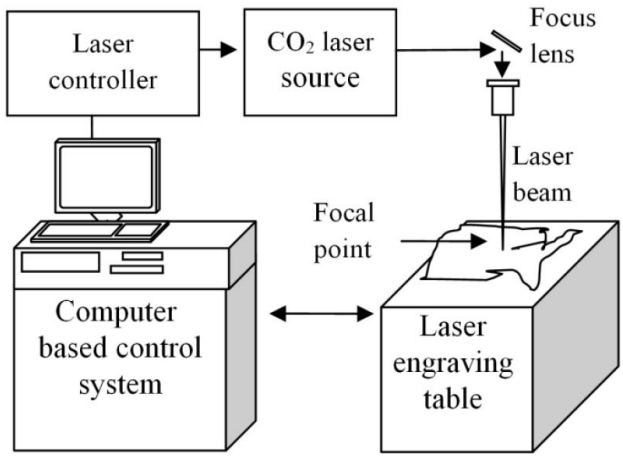

Figure 2.6 Schematic diagram of an experimental setup for laser treatment (Yuan et al., 2012)

Fig. 2.6 shows that a CO_2 laser system contains a CO_2 laser with a set of lenses for directing and concentrating the laser beam onto the fabric and a computer system to regulate the laser beam. Here, the head of the laser can move in horizontal or vertical directions (Yuan et al., 2012).

2.2.4 Applications of laser technology in fashion and textile design

CO_2 gas lasers are applied widely and successfully in the apparel industry. Particularly, they are used in cutting garment patterns, decoration of the fabric surface, denim fading and leather engraving (Nayak & Padhye, 2016). The laser treatment can help to make such processes more

friendly to the environment by using computerized designs; without chemicals. This increases the possibilities for green fashion design with discrete patterns and textures, satisfying the needs of both consumers and industries (Yuan et al., 2012).

The process of laser cutting involves cutting of the fabric into the desired pattern shape by using a laser. Laser engraving includes removing material from the top surface down to a certain depth, creating detailed surface patterns, color fading, and distinctive texture, while retaining the fabric's characteristics. The control of laser treatment parameters like power, speed, and pixels per inch lets the fabric be engraved without charring or damaging the base structure in any other way (Nayak & Padhye, 2016).

Figure 2.7 (Left) Dress with laser cut applique (Jennifer, W. A., 2014) and (Right) laser engraved leather ("Laser engraving leather: an asset for the fashion and decorating industry," n.d.)

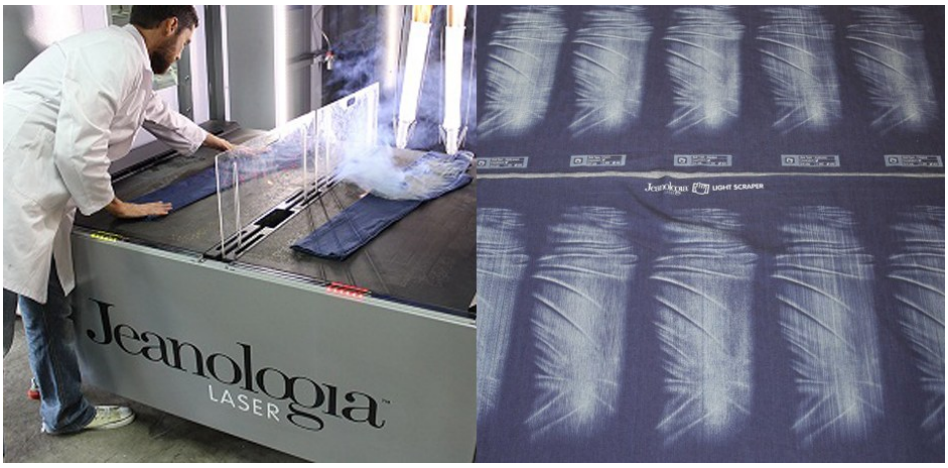

Figure 2.8 Jeanologia's laser engraved denim finishing ("The Denim Industry, At The Intersection Of People, Planet, And Purpose," 2017)

The conventional methods of denim finishing, such as acid washing, sandblasting denim-distressing, and fading, are giving way to the environmentally-friendly laser applications which are growing rapidly (Kan, 2014). Appropriate laser processes make it possible to transfer any image created within a computer-aided design (CAD) software to denim (Nayak & Padhye, 2016).

2.2.5 Laser treatment parameters

The laser treatment process can be influenced by various factors, such as differences in the thickness, density, composition, and material manufacturing processes. The ideal settings to accomplish the desired laser processing effects can be met by controlling real-time laser parameters, like power, speed, and pixels per inch.

The overall energy sent out as laser light per second is laser power (Vilumsone-Nemes, 2018). A laser with higher wattage can burn deeper and lower power can burn shallower, and the laser power level is adjusted from 0 to 100%. Light materials like silk and light cotton may be processed with a 10-30W laser beam, and the majority of textile materials may need 60–100W lasers. And yet, some materials such as Aramid (Kevlar) are processed with 400W laser beams (Vilumsone-Nemes, 2018).

The speed of the laser determines the maximum rate of travel of the laser on the surface and enables a user to choose processing speed from 0 to 100%. While lower speed increases time and burns deeper, higher speed decreases time and burns shallower, which in turn diminishes detail (Universal Laser Systems, 2010). Laser speed must match its power, cut elements' shapes, thickness, absorption features, and material microsurface. For ensuring high cutting accuracy, complicated geometry must be cut using decreased cutting speed (Vilumsone-Nemes, 2018).

When vector cutting, setting pulses per inch (PPI) from 1 to 1000 PPI enables selection of the pulsing frequency of the laser pulse stream applied to the material and controls the number of laser pulses the laser cartridge will emit per linear inch. If the PPI settings are higher when cutting, it may lead to more melting, burning, or charring on the edges. On the other hand, if the PPI settings are lower, it may diminish this effect and may cause decreased details and an edge that looks serrated. A PPI setting between 300 to 500 PPI is a good general value for most applications, but there need to be some experimentation to optimize this setting for a specific material (Universal Laser Systems, 2010).

2.3 Digital Printing of Textiles

2.3.1 Introduction to Digital Textile Printing Technology

The non-contact technology that utilizes nozzles to spray ink drops into precise positions to create a printed design on a textile substrate is known as digital inkjet textile printing (Cie, 2015). Digital inkjet printing involves directly transferring a design onto the fabric from a computer file, without requiring any screen production or exploiting complex machinery (Kan & Yuen, 2012).

A "process" method is used to mix colors; in other words, inks are not premixed but mixed as needed from combinations of distinct ink colors (Cie, 2015). Inkjet printers are provided with primary-colored inks of cyan, magenta, yellow, and black (CMYK), improved by other colors

from individual ink reservoirs (Raymond, 2006). For expanding the printable color space, orange, green, violet, or blue can be utilized, and for enhancing the tonal features, light cyan, light magenta, and grey or light black can be used. The process colors in the printed design are formed by merging the colored ink droplets on the pretreated surface of the textile (King, 2013).

The process enables a wide range of colors in a single printed image along with shade gradients in color or between several colors (Cie, 2015). The style that results after this process can be a replica of images or an artist's original piece, no matter made by hand and then scanned, or created using computer software (Cie, 2015) (Figure 2.10). Nonetheless, there is a limitation imposed on the printable color space by using process colors in inkjet printing compared to the premixed spot colors that are utilized in traditional screen printing of textiles (Cie, 2015; Horrocks & Anand, 2000).

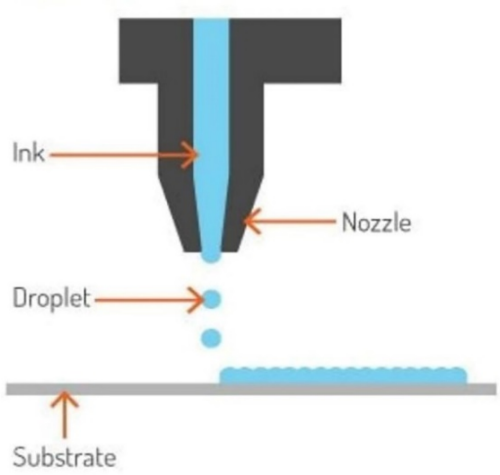

Figure 2.9 Inkjet Printing: Spraying Ink Droplets onto a Substrate ("Thermal Printers vs. Inkjet Printers," n.d.)

2.3.2 Applications of digital textile printing in fashion and textile design

Textiles are one of the digital printing fields which are increasing rapidly, with applications most commonly in apparel, furniture, soft signage, and flags (Lee, 2018). The main printing

technology used in the past was flat and rotary screen printing. The process was hostile to the environment, due to water contamination from chemicals in the dye, and lengthy taking 3 to 4 months. On the other hand, the use of digital textile printing decreases manufacturing time to 1 to 2 weeks. Just-in-time printing, mass customization, and risk reduction in terms of time and inventory are some of the advantages of digital textile printing (Lee, 2018).

For digital inkjet printing, digital camera capture or scanning can be used to generate the digital format needed to make a pattern and to create a design on CAD technology. Design information can be saved in a manner that is readily retrieved and modified, and hence quick pattern changes and design file coloration are achieved. Furthermore, before printing, a textile design can be engineered within the shape of the product (Figure 2.11), and it is possible to specify the required lengths of printed fabric as per individual specific orders (Choudhary, 2018).

Figure 2.10 Susan Wagner's designs at Epson's Digital Couture event ("How Digital Printing Technology Is Taking Us Closer To Fully Customizable Clothing," 2017)

Figure 2.11 The finished marker filled in with the textile design (Chapman, L. P., & Istook, C., 2002)

2.3.3 Digital Textile Printer Classification by Structure

Two types of printing structure which represent distinct methods of handling materials are to place the fabric on a flatbed, either as a cut length or ready-made into a garment, and to continuously supply the fabric by pulling through from the roll (Figure 2.12).

Figure 2.12 (Left) SHIMA SEIKI's Flatbed Textile Printer SIP-160F3 ("Shima presents its digital textile printing offering," 2017), and (Right) HP's Latex 335 Roll-to-roll Textile Printer ("HP LATEX 115 PRINTER", n.d.)

For holding fabrics in place, the flatbed printer is equipped with an even surface with a vacuum device which offers suction beneath the bed. This sort of printer is mainly utilized for printing cut-pieces of fabric individually (Ayau, 2018). It is possible to print patterns along the

length or as a “placement” print in a particular location and on a ready-made item, like a T-shirt. The other type of printer is the roll-to-roll printer that is an entry-level printer exploiting a series of pinch rollers, grit rollers, and a small motor for moving the fabric (Ayau, 2018). It is called “roll-to-roll” since, to move through the printer, a fabric roll releases a fabric length that is then printed and wound onto another roll, prepared to be stored, transported, and used.

2.3.4 Classification of Ink Colorant

To choose colorant type, fiber content and the fabric’s ultimate use should be considered, along with which pretreatment is compatible with the fabric and colorant. Textile printing inks are of five main types, which are formulated for compatibility with the inkjet process. Inks must be matched to fabrics considering fabric structure or use and fiber content (Cie, 2015).

Additionally, there are two kinds of inks used to print on textiles: dye and pigments (Lee, 2018). Dyes are susceptible to being dissolved in water or fluid and used for coloring textiles, basket reed, and other materials which are permeable to fluids. On the other hand, to produce colorant, pigments don’t dissolve but rather are suspended in a carrier fluid as tiny particles (Lee, 2018). Inkjet formulation components differ in their detail but in general contain a colorant, solvent (carrier), water, surfactant, acid, or alkali (Cie, 2015).

2.3.4.1 Reactive dyes inks

Reactive inks can be utilized on the widest variety of fiber contents, including cellulosic, protein, and synthetic nylon. They are most efficient for printing on fabrics that are derived from plants and are cellulose-based, like cotton, linen, rayon, hemp, or jute, in which they create bright shades with remarkable colorfastness to washing and light (Lee, 2018).

They are referred to as reactive inks because they permeate the fabric and react with the fiber and the pretreatment chemicals under alkaline conditions to build a covalent chemical bond

between the ink and fiber (Hawkyard, 2006; Lee, 2018). Pretreatment of fabrics is required before they are printed and steaming, washing, and drying needed after printing (Lee, 2018).

2.3.4.2 Acid dyes inks

Acids are used to produce and apply acid dyes, which are renowned for printing not just protein fibers, such as wool and silk, but also nylon (Cie, 2015). They are anionic dyes that can be soluble in water and have no reaction with the fiber for structuring covalent bonds, but rather, they are drawn to spaces on the fiber that are charged positively. Often, the shades obtained are deeper and brighter as compared to those of reactive dyes (Cie, 2015). To avoid wicking of the ink on the fabric, a pretreatment is needed; for fixing the dye after printing, steaming is required (Chen et al., 2002; Yang & Li, 2003).

2.3.4.3 Disperse dyes inks

Synthetic fibers like polyester, lycra, and spandex that have low water-absorption receive disperse dyes as finely dispersed particles. Disperse dye inks are produced in two types by the ink manufacturers; for transfer printing and direct printing onto the substrate (Hawkyard, 2006). The inks for transfer printing are a special kind of disperse dye, which is first printed on paper and then transferred to fabrics by using a heat press (Kan & Yuen, 2012). Disperse dye-based inks for inkjet printing have specific properties for fastness and can be printed on the substrate directly. Steam of high temperature is required in post-processing so that the dyes are fixed and give satisfactory print quality and colorfastness (Fan et al., 2008; Lee, 2018).

2.3.4.4 Pigments inks

Pigments are capable of being applied to fiber types or blends that do not have compatibility with dyes: cellulose fibers, protein fibers and nylon (Cie, 2015). Pigments are not soluble in water, and particles are unable to interact with fibers; they are instead mechanically held

or fixed to the surface of fibers by using a polymeric binder as an additional component in the ink (Hawkyard, 2006). The binder forms a film or glue when cured after printing and holds the pigment particles on the fabric in place (Cie, 2015).

Applying pigment ink does not require pretreatment or washing after pigment fixation (Kan & Yuen, 2012; King, 2013). But still, pretreatment can improve the ink receptiveness, color intensity, and color gamut of fabrics (Ding et al., 2019; Lim & Chapman, 2019).

Table 2.1 summarizes four ink types and their features.

Table 2.1 Ink Type and Features (Lee, 2018)

Ink Type	Acid Dye	Reactive Dye	Pigment	Disperse Dye
Fabric	Nylon, wool, silk (protein-based fibers)	Cotton and rayon materials (Cellulose: plant based fibers)	Primarily cotton or cotton mixed fabrics (non-fabric specific)	Polyester and synthetic fibers
Printing Method	Direct to pretreated fabric	Direct to pretreated fabric	Direct-to-fabric	Direct-to-fabric
Characteristics	Dye absorbed by the fabric	Dye absorbed by the fabric	Insoluble pigment adheres to the top of the fabric with a binder	Water insoluble
Post-Treatment	Dry, saturated steam and wash (from cold temperature to hot)	Dry, saturated steam and wash (from cold temperature to hot)	Dry heating (UV or hot air)	High energy calendar (super heated steam) or press (dry heat)
Pros	Bright colors Light fastness (Better than reactive inks) and great wash fastness	Bright colors, light fastness and great wash fastness	In past years color pop was weak	Less wastage then dye sublimation (economical and ecological)

2.3.4.5 Latex Ink

Latex ink is suitable for all fabrics, natural, synthetics, and blended fabrics (Bordeaux Digital Printink, n.d.). Latex Ink consists of a liquid ink vehicle carrying latex polymer and pigment particles to the print media surface (HP, 2011). Through thermal printhead technologies, heat is used to evaporate the water and enable polymers to bind the pigments with the medium (Image Reports, 2014). Upon removing the liquids inside the printer, the printed fabric is

completely dry and odorless, and can be handled, finished and shipped immediately (HP, 2012). Prints can be displayed outdoors or indoors (Pericot, 2016).

2.3.5 Pretreatment and Posttreatment

2.3.5.1 Pretreatment

Certain types of chemicals are applied to the fabrics to prepare for inkjet printing. These chemicals allow the substrates to be receptive to water-based treatments. The pretreatment chemicals can lead to deeper color shade, fixation of dyes and colorfastness, and reduce undue wicking, color migration, and bleeding (Cie, 2015; Fan et al., 2003; Hawkyard, 2006).

The pretreatment formulation is dependent on the type of fiber and ink or their combination. Thickeners, alkalis, urea, and other auxiliaries are the principle and most common components of inkjet textile printing pretreatments (Cie, 2015).

2.3.5.2 Posttreatment

Color fixation to make the inkjet print permanent on the fabric is done as posttreatment. The required fixing process differs based on the pretreatment, the ink type, and the final requirements. The posttreatment process mainly helps to uptake and retain the ink on the textiles (Cie, 2015), and increase the color gamut. For example, many textile dyes create a wider range of colors after steaming. Posttreatment also improves colorfastness to the effects of light, crocking or washing (Campbell, 2006).

After printing, steaming is required for bonding of reactive and acid dyes to the fiber, and heating is required for disperse dye sublimation (Campbell, 2006). Dry-heat curing or fixation is required for pigment inks (Hawkyard, 2006). Washing and drying should follow as the final stage.

2.4 Color Science

2.4.1 Introduction

Color is a perceptual response to light entering the eyes either directly or indirectly, from light sources that are self-luminous or light reflected by illuminated objects (Westland & Cheung, 2006). In figure 2.13, a person's perception of color depends on cone sensitivity, color blindness, age, health, and even attitude (Jordan, 2001). Other influencing factors are color of the surrounding or background, the relative area sizes of contrasting color, and the gloss and texture of a surface (Bae, Hong, & Lamar, 2015).

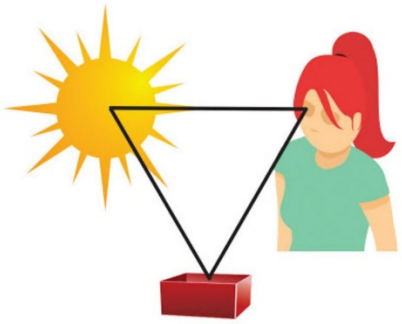

Figure 2.13 Color results from the interaction of a light source, an object, and the eye and brain, or visual system (Berns, 2019).

The nanometer (1 nm = 10^{-9} m) is a unit of length that describes the wavelength of the light, which is a form of energy. The colorimetric properties of an object are characterized by its reflectance or transmittance when light falls on it. In the case of transparent material, a portion of the light is transmitted through and gets out on the other side (Westland & Cheung, 2006). The characteristic of reflection is most important in colored objects that are opaque or translucent (Choudhury, 2014a).

The color of the material is determined by the amount of light reflected throughout the visible range of the spectrum (Choudhury, 2014a). The range of wavelengths of visible light is from 380 to 780 nm in the human system of vision, with red having the longest wavelength of 780

nm with the lowest frequency (Figure 2.14). The shortest wavelength of about 380 nm with the highest frequency is the color violet.

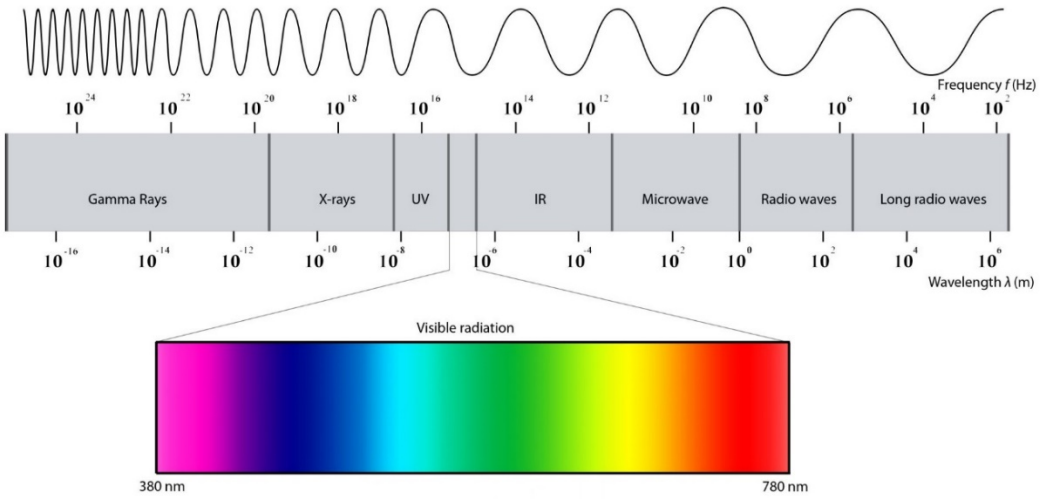

Figure 2.14 The Range of Visible Radiation from 380 nm to 780 nm, which is part of the Electromagnetic Spectrum (Durmus, 2017)

Light is said to be reflected when it scatters back from opaque materials (Choudhury, 2014a). An object's geometry, material, geometric surface attributes, and spectral distribution of the incident light along with its shape affect the light reflected from it (Dorsey, Rushmeier, & Sillion, 2008). Light scatters or gets absorbed inside the material when it is not reflected.

The phenomenon of dispersing the light in various directions called diffuse reflectance takes place on rough surfaces. On the other hand, smooth glass-like surfaces produce specular surface reflectance in which the angle of reflection equals the angle of incidence of illumination and with opposite signs (Berns, 2019) (Figure 2.15).

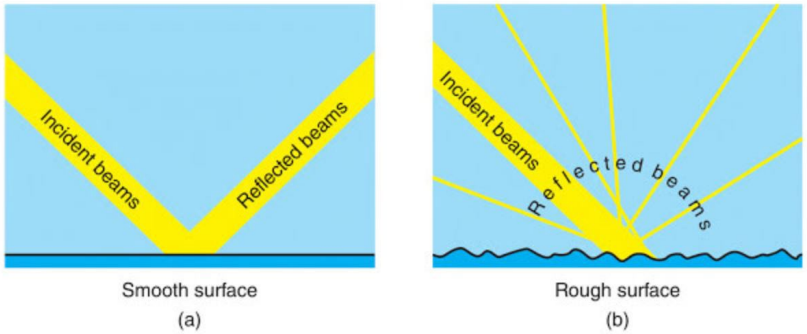

Figure 2.15 Incident light reflecting from smooth and rough surfaces (Berns, 2019)

2.4.2 Visual and Instrumental Color Assessment

In visual assessment, chromatic attributes and diverse geometric variables, like shape, texture, and direction can be perceived by an observer at the same time. Instruments that are presently available have not yet advanced to such versatility since just one attribute can be measured at one time by them (Choudhury, 2014a). Nonetheless, visual assessments are primarily qualitative, subjective, and contextual (Choudhury, 2014a). Judgments about the degree of differences in perception between two colored samples, or whether a batch can be accepted as a match to the standard, vary significantly across individuals.

The visual assessment procedure can be supported by instrumental assessments that are less varied because they offer a way to consistently quantify distinctions of color more rapidly and reproducibly, and hence enable product color tolerances to be managed. Furthermore, differences indistinguishable to the human eye can be captured by tools, such as colorimeters and spectrophotometers (Choudhury, 2014b). Sectors utilizing color extensively, like textiles, coatings, plastics, graphic arts, and imaging exploit instrumental color measurement systems. Particularly, one of the most significant applications is color quality control using color-difference formulas that are designed to quantify variations in color between sample pairs (Choudhury, 2014b).

2.4.3 Spectrophotometer

To measure the interaction between a chemical compound such as dye or pigment on a textile sample and electromagnetic radiation, spectroscopy or spectrochemical analysis can be used (Choudhury, 2014a). A sample is illuminated by spectrophotometers to measure the amount of light that is reflected or transmitted at discrete wavelengths. Spectrophotometers deliver a voltage signal; this signal differs as there are changes in the amount of light absorbed by the object. A sample's measured signals (absorbance) offer wavelength by wavelength spectral reflectance or transmission data without any human translation (Choudhury, 2014a).

It is possible to calculate and manipulate psychophysical or colorimetric data through spectrophotometer/computer combinations (Figure 2.16). Here, differences in color are immediately shown in numerical terms utilizing L*a*b* or L*C*h values, and the acceptability of the sample is determined based on tolerance limits (Choudhury, 2014b).

Figure 2.16 Datacolor 800 Spectrophotometer and Textile Color Matching Software ("Datacolor match textile," n.d.)

2.4.4 Spectral Reflectance Curve

Spectrophotometers are used to measure the reflectance (or transmittance) value of a compound on a sample as a function of electromagnetic radiation under defined lightning and geometric circumstances. In particular, the reflectance value indicates the proportion of the magnitude of reflected light to the magnitude of light which falls on a colored surface at each wavelength (Berns, 2000).

As shown in Figure 2.17, the group of reflectance values produces a visual curve, referred to as the spectral reflectance curve, for opaque material. On the other hand, for transparent materials, the impact of an object on light can be defined by its spectral transmittance curve (Berns, 2000). The spectral reflectance (or transmittance) curve provides information about the color properties of the surface in detail and is utilized to identify and communicate color (Hunt, 2005).

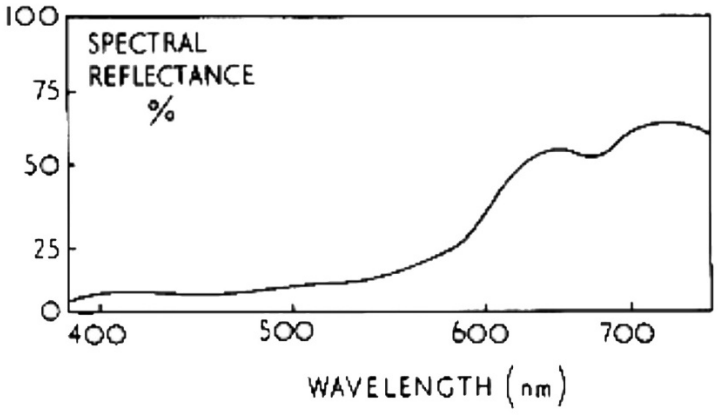

Figure 2.17 Reflectance Curve of a Red Color (Hunt, 2005)

2.4.5 Attributes of Color

Color perception relies on a specific relationship between physical stimulus properties and a sensation's subjective interpretation. Color perception can be identified in terms of three properties even though it depends on many more than three stimulus parameters. Hue, saturation and lightness are the three properties or psychological attributes of color. These are primarily

related to the stimulus dimensions of the dominant wavelength, spectral purity, and luminance respectively. Changes in one stimulus variable may affect all three psychological attributes of color (McDonald, 1997).

2.4.5.1 Hue

The definition of hue is a feature by which an area is visually perceived to be similar to one of the colors red, yellow, green, and blue, or to a combination of pairs of colors that are adjoining in a closed ring (Hunt & Pointer, 2011). The definition of hue implies that it is the variable one experiences when looking at a Munsell (or other system's) hue circle with their sequence offered by a spectrum (Figure 2.18). In 1905, Munsell proposed three psychological attributes (hue, value, and chroma) that have become generally accepted for object colors (Figure 2.18) (Choudhury, 2014a).

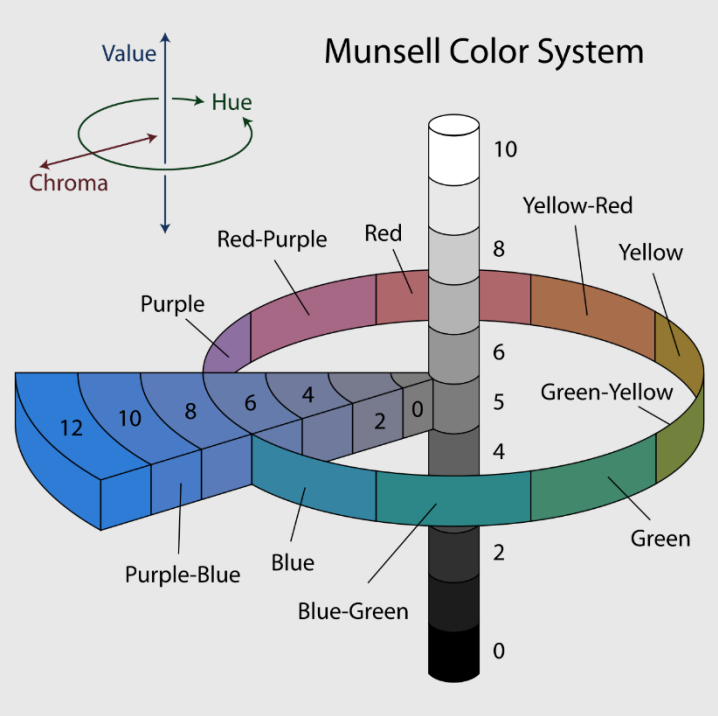

Figure 2.18 Munsell Color System (Choudhury, 2014a).

2.4.5.2 Lightness and Brightness

Lightness is regarded as equivalent to one of a series of grays ranging from black to white. Also, it depicts the surface appearance and has no dependency on adaptation and illumination (ASTM E284; Choudhury, 2014a). Brightness is the intensity of light sources, which is a characteristic of visual perception following which a region is perceived to display more or less light. A different perception of brightness may be produced by the same source at a different time, as the sensation is dependent on adaptation (Hunt & Pointer, 2011). Lightness is the perceived brightness of an object that is not white in comparison to that of an object that is white under identical illumination (Hunt & Pointer, 2011).

2.4.5.3 Colorfulness, Chroma, and Saturation

According to colorimetry and color theory, the concepts of colorfulness, chroma, and saturation are associated but also distinct in terms of a color's perceived intensity (Choudhury, 2014a). A given area appears to show its hue more or less per an attribute of visual perception called colorfulness (Hunt & Pointer, 2011). Colorfulness refers to chromatic power perceived regardless of the magnitude. The achromatic colors that can indicate zero colorfulness are white, true gray, or black. Chroma can also be taken as the color attribute that indicates the degree by which the color is away from the grey of the same lightness (ASTM E284). The colorfulness of an area compared in proportion to its own brightness and not requiring any similarly illuminated white is saturation (Hunt & Pointer, 2011), while the colorfulness relative to the brightness of another color that appears white under a similarly illuminated area is chroma (Choudhury, 2014a).

2.4.6 CIE L*a*b Color Space

The science and technique for quantifying and physically describing color perception by humans is called colorimetry (Ohno, 2000). The Commission Internationale de l'Eclairage (CIE)

defined primary tristimulus values, which are the three numbers that specify colors numerically for a standard observer response. In 1976, the CIE specified the formula CIE L*a*b, which is a three-dimensional uniform color space that provides an accurate specification of object colors and color differences (Luo, 2006). The basis of the formula is the Munsell visual color order system (Choudhury, 2014b) (Figure 2.19).

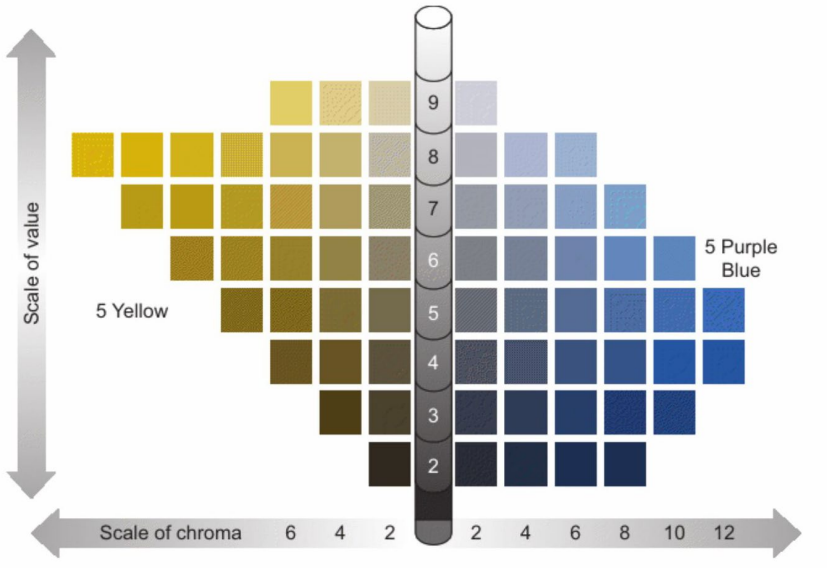

Figure 2.19 Munsell Value Chroma charts for 5 Yellow and 5 Purple Blue Munsell Hues (X-Rite)

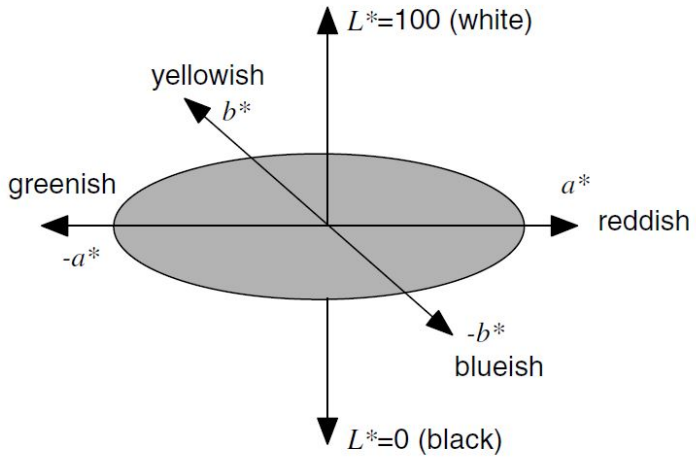

Figure 2.20 CIE L*a*b color space (Ohno, 2000)

In CIE L*a*b space, L* denotes the lightness, and a*, b* are the hues, as shown in Figure 2.20, with the value scale located in the center of the color space. The L* value of 0 represents a reference black, and 100 represents a white, the value of a* denotes the redness–greenness, and the value of b* denotes the yellowness–blueness attributes (Luo, 2006).

CIE L*a*b quantifies and calculates the plotted coordinates of the difference in color between two sample objects or the sample and a standard (Berns, 2000). These differences between a standard and a sample are defined by their differences in values of lightness (ΔL*), chroma (ΔC*), redness-greenness (Δa*), yellowness-blueness (Δb*), and the total difference in color between the two samples are represented by Euclidean distance (ΔE^*_{ab}):

$\Delta L^* = L^*_{batch} - L^*_{standard}$ = difference in lightness and darkness (+ = lighter, - = darker)

$\Delta C^* = C^*_{batch} - C^*_{standard}$

$= (a^*_{batch}{}^2 + b^*_{batch}{}^2)^{1/2} - (a^*_{standard} + b^*_{standard})^{1/2}$ = difference in chroma

$\Delta a^* = a^*_{batch} - a^*_{standard}$ = difference in red and green (+ = redder, - = greener)

$\Delta b^* = b^*_{batch} - b^*_{standard}$ = difference in yellow and blue (+ = yellower, - = bluer)

$\Delta E^*_{ab} = [(\Delta L^*)^2 + (\Delta a^*)^2 + (\Delta b^*)^2]^{1/2}$ = total color difference between the two samples

Positive differences denote that the batch varies more from the standard in one or more of L*, a*, b*, or C*. Larger positive differences show more color differences.

2.4.7 Kubelka-Munk Theory

The Kubelka-Munk (K-M) theory is used by the textile industries to identify the quantity of colored dye in printed or dyed fabrics (Kang, 2006). The equation denotes the association between the measured reflectance values of a layer, *R*, and dye concentration and is used to

calculate the value of the color strength (Baumann et al., 1987). The theory was created by Kubelka and Munk to model the light that emerges from a translucent or opaque object.

$$K/S = (1-R)^2 / 2R$$

and the inverse relationship

$$R = 1+K / S - \{ (1+K/S)^2 - 1 \}^{0.5}$$

Here, the absorption coefficient of a colorant is denoted by *K* and the scattering coefficient by *S*. It is deduced that there is an increase in color strength with the increase in absorption (Lim & Chapman, 2019). If one triples the dye concentration, the values of K and S triple. The sum of the K/S values in the visible region of the color spectrum in the Kubelka-Munk equation denotes the color strength (Baumann et al., 1987).

The theory also refers to mixtures of colorants and states that the K/S value for multiple dyes is the sum of the K/S values of the individual colorants (HunterLab, 2008), as follows:

$$(K/S)_{mixture} = a(K/S)_{colorant\ 1} + b(K/S)_{colorant\ 2} + c(K/S)_{colorant\ 3} \ldots + (K/S)_{base}$$

a, b, c, etc. are the concentrations of the corresponding colorants.

The parameter K/S is a constant parameter, and it is possible to utilize this relationship to decide the strength of the dyeing depending on the degree of absorbance of the surface, which in turn is related to the amount of dye applied. The function can also be used to acquire color matching formulations based on a mixture of dyes (Shamey, 2018).

CHAPTER 3: METHODOLOGY

3.1 Research Objective and Research Questions

The research objective is to determine if creating pile height variation by laser engraving cotton velvet fabric prior to digital inkjet printing can impact the resulting color. There are two research questions: [1] Does pile height variance created by treating at differing laser intensities result in instrumentally measurable differences in color properties based on pile height? [2] Does pile height variance created by treating at differing laser intensities result in instrumentally measurable differences in color properties based on printed color?

3.2 Research Design and Workflow

In the research study, laser engraved and then digitally printed fabric samples were developed, and a spectrophotometer used to measure color properties of the printed colors on the samples.

An investigation was developed to examine if laser engraving on a white cotton velvet could influence the color consistency of the digitally printed color. A printing pattern was designed, containing seven solid stripes, each with a different color: cyan, magenta, yellow, black, red, green, and blue. Four 100% cotton velvet substrates with different pile heights were created by laser treatment from one base cloth, controlling laser intensity with the percentage of grayscale in a graphic. The overall process flow for this research is represented in Figure 3.1.

Following the pilot investigation, four research stages were identified: (1) apply laser engraving on the velvet fabric; (2) digitally print on the laser engraved fabric; (3) measure color properties of the printed colors samples with a spectrophotometer; (4) statistically analyze and interpret the data.

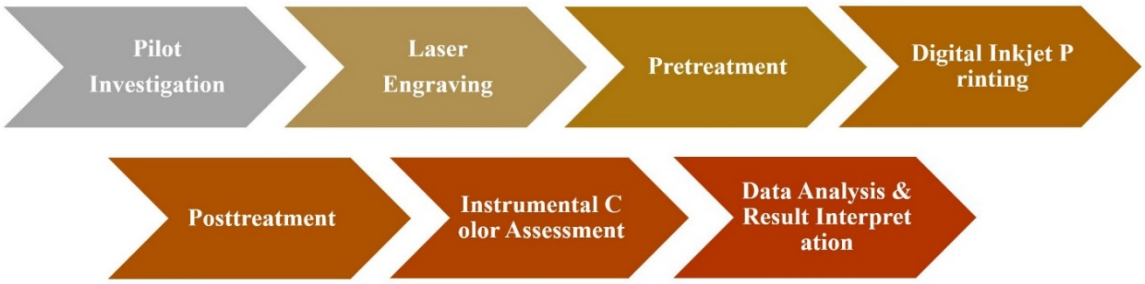

Figure 3.1 Entire Workflow of Research Methodology

3.3 Pilot Investigation

Before launching final sample development, pilot experiments were conducted to determine optimal settings for pile height variation and color fixation onto the velvet fabric. The following sections describe the pilot work steps to create samples for evaluating color consistency.

3.3.1 Material

White cotton velvet fabric donated by jb martin was selected as testing material for the pilot investigation. The material was a 100% cotton velvet without any additional treatment. It had 6.7 oz./square yard (226 grams/square meter). Width and length of the fabric was 60 inch and 165 inches.

3.3.2 Scouring

The velvet pile was lying down to the base cloth, and the fabric was scoured to make the pile stand up and remove any dirt or stain. Water direction and machine input direction were marked to make the pile stand straight by applying the water force. The velvet fabric was scoured in a washing machine with 50g of soda ash (sodium carbonate), and 50g of Clarite® ONE-AM in 50L water. The washer was set to a hot/cold cycle with an extra rinse for removal of the bubble caused by residual soda ash and Clarite® ONE-AM.

3.3.3 Laser Engraving

Several pilot experiments were executed to set a range for the laser engraving parameters including the power, and speed of the laser and PPI (pulses per inch) of the testing file graphic. The goal was to avoid destroying the integrity of the fabric foundation and achieve an obvious visual effect.

A UNIVERSAL VLS6.60 pulsed CO_2 laser machine (Figure 3.2) was utilized along with the computer-controlled software called the Universal Control Panel (UCP) to apply laser engraving on the cotton velvet fabric. The size of the focus lens was 2.0 inch. The laser option was 40 Watts, which generated a wavelength of the laser beam of 10.6 μm, and the power requirement was up to 110V/10A.

Figure 3.2 UNIVERSAL VLS6.60 CO_2 laser machine (Universal Laser Systems, 2017)

A testing file was created, and it is represented in Figure 3.3

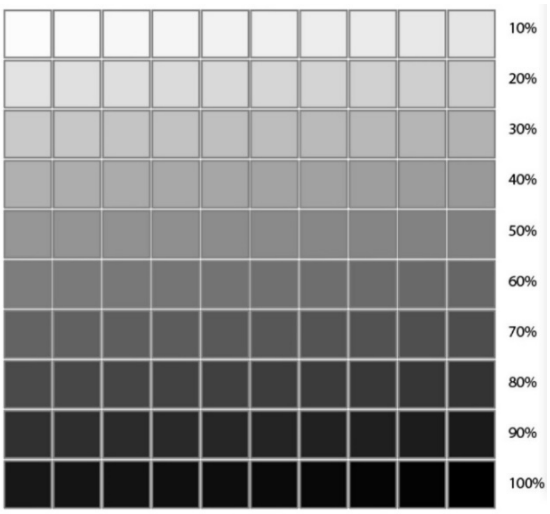

Figure 3.3 A Grayscale Testing File for Laser Engraving

In the testing file, the color of each square was increased by 1% blackness so that the first square was just 1% black and the last square was 100% black. Each row was ten squares, so comparing the tiles at the end of each row gave a 10% change. The laser cutting machine engraves at the power the user sets for the pure black graphics and uses less density of dots in different levels of the gray graphic to achieve more or less removal of material.

In the Universal Control Panel (UCP) software (Figure 3.4), the user can control the laser engraving parameters, including the power and speed and PPI (pulses per inch) of the laser. Using the testing file, the velvet fabric was engraved by applying laser power 30% to 100% with each step of a 5% increment. For the speed setting of laser, 100% was consistently maintained in all trials for time efficiency. 300, 400, and 500 pulses per inch (PPI) were applied because a PPI setting between 300 to 500 is a good nominal value for most applications (Universal Laser Systems, 2010).

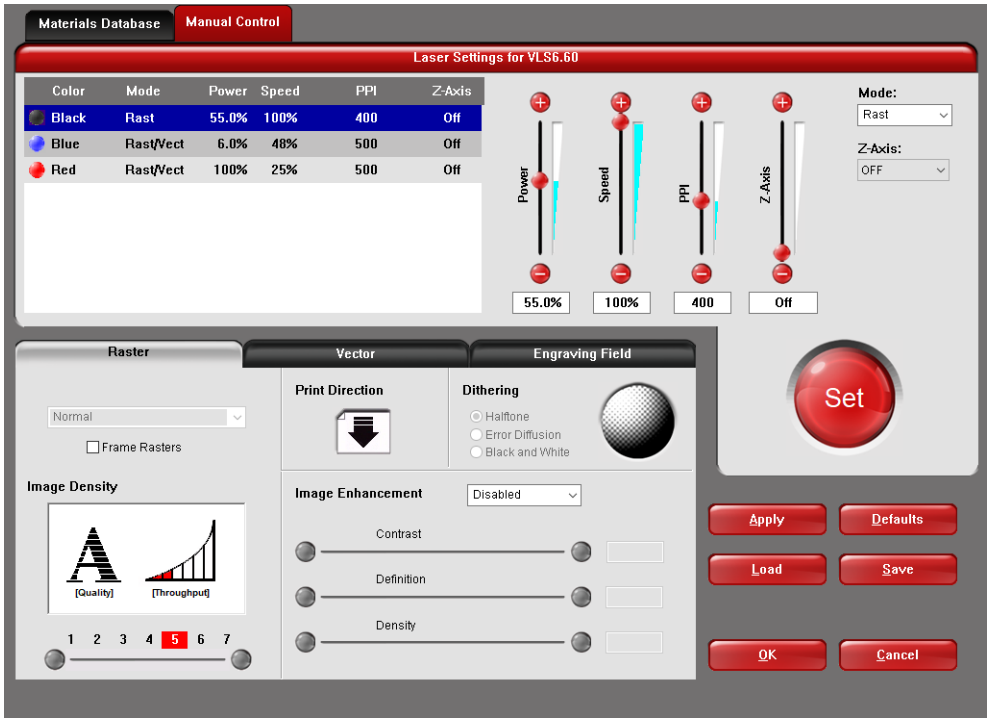

Figure 3.4 Manual control in the Universal Control Panel (UCP) software

As seen in Figure 3.5, the laser-engraved squares on the white cotton velvet fabric started to turn into brownish-yellow from some point of grayscale percentage. The fabric started to be destroyed by applying 60% power. The influence of PPI setting 300, 400, and 500 to the laser engraving quality wasn't observed with the unassisted eye.

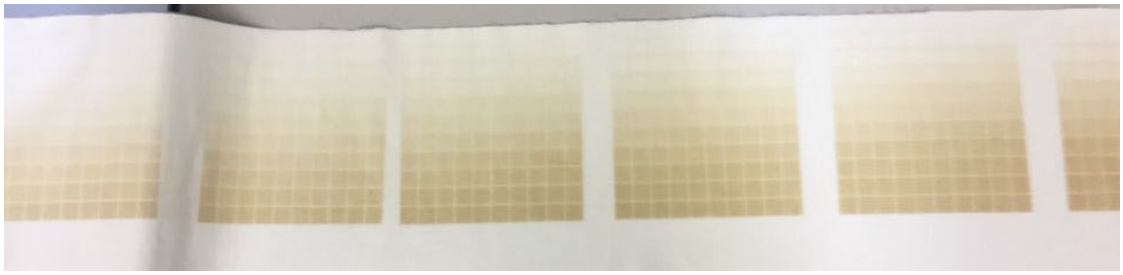

Figure 3.5 Image of Laser Engraved Velvet Fabric with Each Step of 5% Laser Power Increment

As a result, the laser power setting was fixed at 55% because the integrity of the cotton velvet fabric structure started to be destroyed from 60% power. For pile height variation, laser

intensity was controlled by using 0%, 25%, 50%, 75%, and 100% grayscale patterns to maximize pile height and surface contour variation. Laser speed 100% and PPI 400 settings were maintained settings for all sample development.

After laser treatment, the fabric was washed by hand in cold water mixed with two drops of synthrapol® surfactant to remove yellowish residues. After washing, the sample was located on a clear table in a ventilated room for twenty-four hours to dry naturally.

3.3.4 Pretreatment

The fabric was pretreated to assist the absorption and retention of ink in preparation for inkjet printing and for improved color quality and saturation without bleeding and color migration. The Shima Seiki SUM 100 pretreatment machine sprayed (Figure 3.6) the pretreatment liquid onto the fabric with a nozzle system.

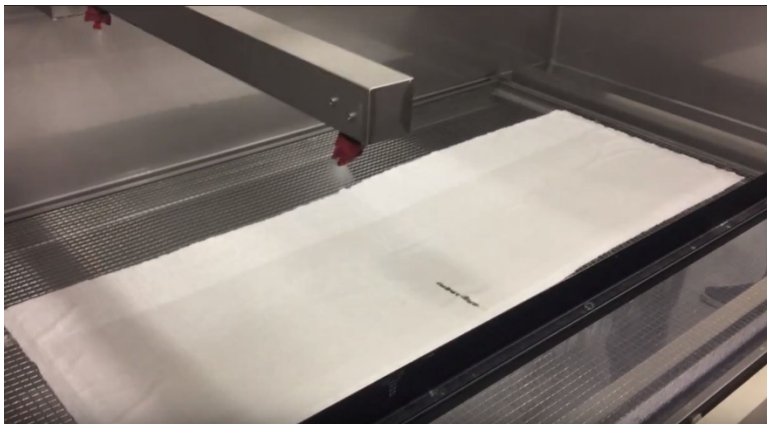

Figure 3.6 Shima Seiki SUM 100 pretreatment machine

For the pretreatment liquid preparation, one kilogram of the Shima Seiki pretreatment powder was stirred in eight liters of 68 degrees Fahrenheit water until dissolved and antiseptic for pretreatment was mixed. Then the pretreatment liquid was left for twelve hours until it was dissolved completely. After twelve hours, the liquid was filtered with gauze just before using it. The fabric was dried for twenty-four hours after pretreatment.

3.3.5 Digital Inkjet Printing

Following pretreatment, seven solid colors: cyan, magenta, yellow, black, red, green, and blue were printed in 1.5” × 1.5” squares on the surface of the pretreated fabric with a Mutoh ValueJet 1938TX roll to roll printer. Width of the roll fabric was 63”. Aligning the printing properly within the 32” width 18” length laser engraved region of the sample was demanding. So, the printing file was modified to continuous vertical stripes in the second trial. Some ink smudges and bleeding were observed during printing, and a different pretreatment formulation was applied in the third trial for better ink fixation.

3.3.6 Steaming

The printed fabric was steamed with the Shima Seiki SSM 100 flatbed steamer for twelve minutes at 97 degrees Fahrenheit to secure the dye-based inks as a permanent feature onto the fabric. In the first trial, the printed fabric was steamed right after printing. In the second trial, the printed fabric was steamed after twenty-four hours to dry the surface so that inks would not become smeared. Once steaming had completed, the fabrics were located on a clear table in a ventilated room to dry naturally before washing.

3.3.7 Washing

After steaming, the fabric was washed to remove any dye molecules unfixed to the fabric, accumulated unwanted matter, and pretreatments. In the first trial, the fabric was washed by hand in warm water mixed with two drops of synthrapol® surfactant in a metal bucket five times. In the second trial, the fabric was machine washed in 16 liters of water for twenty-five minutes. Oxidizing agent powder (4g/L), soda ash (2g/L), and Apollo scour SDRS (2g/L) were added in the water.

Excess ink and migrated smudge on the surface were not cleaned enough in the hand-washed fabric in the first trial. Machine-washing, the fabric in the second trial, was able to remove

the residual smudges significantly, but the color was not as saturated as the hand-washed fabric from trial 1.

3.3.8 Conclusions from Pilot Investigation

In the laser engraving stage, 0%, 25%, 50%, 75%, and 100% grayscale at 55% power and 400 pulses per inch were selected to control the laser intensity and modify pile height and surface contour of velvet fabric without structure destruction. Pile removal left residue. As more pile was removed, the more residue remained and more discoloration was marked.

The pretreatment machine and the chemical used in the pilot investigation are intended for printing on knitted fabrics or garments, and were not that effective for pile fabrics. Some migrated ink smudges were observed during printing or after steaming, and additional trials with different conditions in steaming and washing were executed. Many ink smudges could be removed after machine washing, and ink fixation on the surface after washing could be improved by using a pretreatment formulation called PREPAJET® provided by Huntsman.

3.4 Final Sample Development

3.4.1 Material

White boiled off 100% cotton velvet yardage without a finish donated by Cotton Incorporated was utilized for final sample development. It was 12.738 oz./square yard (431.6 grams/square meter), and 1628.8 μm pile height.

3.4.2 Research Stage 1: Laser engraving on cotton velvet fabric

Because of the malfunction of UNIVERSAL VLS6.60 (Universal Laser Systems, Inc.) at Wilson College of Textiles, laser engraving for the final sample was outsourced from Ostling's Laser Craft (Raleigh, NC). A Fusion 32 (Epilog Laser) 60 Watt CO_2 laser machine (Figure 3.7) engraved a 32” by 20” dimension file (Figure 3.8) on the cotton velvet fabric perpendicularly to

the selvage direction. The technical specifications of the laser machine are given in Table 3.1. A graphic file for one sample contained 25%, 50%, 75%, and 100% grayscale stripes (Figure 3.8), and two samples were produced.

Figure 3.7 Fusion 32 (Epilog Laser) 60 Watt CO2 laser machine

Figure 3.8 A File of 25%, 50%, 75%, and 100% Grayscale for Laser Engraving

In a graphic file (Figure 3.8), the laser machine engraves at the power the user sets in 100% black and removes less material in the lower level of the gray graphic (25%, 50%, and 75% grayscale). As a result, 100% black regions will have the shortest pile depth and vice versa. After several tries, 70% power 100% speed 400 PPI setting was chosen to avoid weakening the fabric foundation to where it would rip if the pressure were applied with a finger.

Table 3.1 Technical Specifications of Epilog Fusion 32 Systems

Engraving Area	32" x 20" (812 x 508 mm)
Maximum Material Thickness	14" (101.5 mm)
Maximum Speed	165 inches/second
Laser Source	60 Watt, CO2, air-cooled, all-metal Waveguide laser tube, 10.6 micrometers.
Print Driver and Software	Laser Dashboard, Epilog Control Center, and Epilog Job Manager.
Operating Modes	Optimized raster, vector, or combined modes with engraving and cutting in one job.
Size (W x D x H)	52.5" x 35.5" x 40.75" (1334 x 851 x 1035 mm)
Weight	500 lbs (227 kg), Dual Source: 536 lbs (243 kg)
Electrical Requirements	Auto-switching power supply accommodates 110 to 240 volts, 50 or 60 Hz, single phase.
Laser System Classification	Class 2 Laser Product - 1 mW CW Maximum 600-700 nm.

Figure 3.9 A Laser Engraved Result for 25%, 50%, 75%, and 100% Grayscale File (Left), A Kettle Used for Washing (Right)

After laser treatment, the engraved parts of fabric turned into brownish yellow (Figure 3.9) caused by thermal oxidation of cellulose fibers, and the fabric was washed because the discoloration can influence the digitally printed color quality. The samples were washed twice in cold water by hand in a kettle to remove yellowish residues. After washing, the samples were spun in a Bock Centrifugal Extractor and dried in Kenmore Elite dryer for 30 minutes with the medium temperature setting. Images of the Bock Centrifugal Extractor and Kenmore Elite dryer are show in Figure 3.10. Wrinkles created during the washing and drying process were ironed from the back after the fabric was dried thoroughly (Figure 3.11).

Figure 3.10 Dryers Used for Washing after Laser Treatment (a) Bock Centrifugal Extractor; (b) Kenmore Elite.

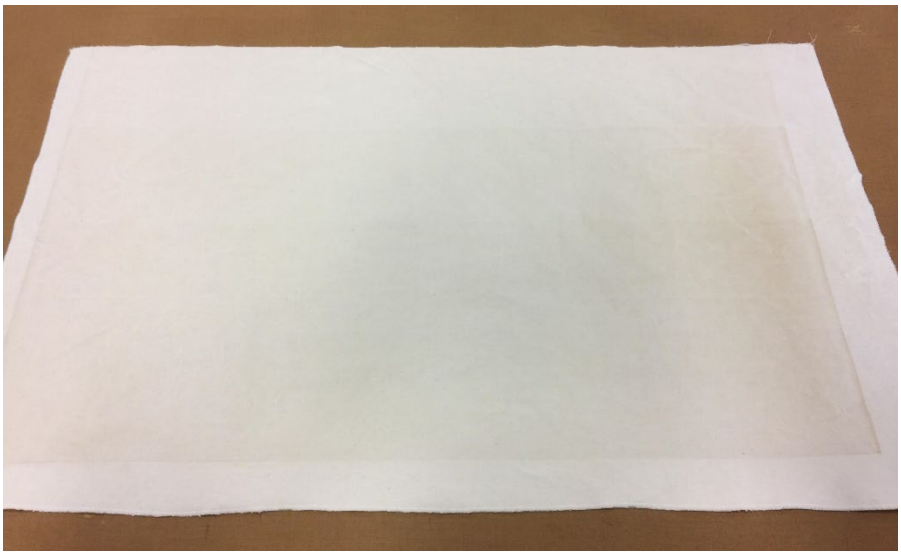

Figure 3.11 Laser Engraved Sample after Washing, Drying, and Ironing

3.4.3 Research Stage 2: Digital Inkjet Printing on the Laser Engraved Fabric

3.4.3.1 Pretreatment

Two laser engraved samples and an untreated (control) sample were pretreated to ensure that the print clarity (Tyler, 2005), color, and brightness, as well as the colorfastness performance, were at a high level (Horrocks & Anand, 2000).

To improve migrated ink smudges after inkjet printing seen in the pilot investigation, a pretreatment formulation called PREPAJET® provided by Huntsman (Hider, 2018, pp. 48-49) was applied. The pretreatment chemical calculation and wet pick up percentage of the cotton velvet fabric are shown in Table 3.2.

Table 3.2 Pretreatment Chemical Calculation

Chemical/Name	Volume/Mass	Calculation
Wet Pick Up %	{(42.34 g – 20.71 g)/20.71 g} x 100 = 104.44 %	
Weight of an 8.5” x 8.75” Fabric (Dry)	20.71 g	
Weight of an 8.5” x 8.75” Fabric (Wet)	42.34 g	
Weight of Total Bath	10 L = 10,000 mL = 10,000 g	
Total Weight of Three Samples	793.7 g ≒ 1000 g	
Water	10,000 g – (1000 + 1000 + 400) = 7600 g = 7600 mL	
Huntsman Prepajet PIJ (Alginate)	100 g/L	100 g/L x 10 L = 1000 g
Urea	100 g/L	100 g/L x 10 L = 1000 g
Soda Ash	40 g/L	40 g/L x 10 L = 400 g

The pretreatment solution was prepared and mixed in a plastic bucket, and the three samples were submerged in the solution at the same time. After applying physical pressure for

enough saturation, the samples were passed through a Mathis HVF model padding machine set to 20 psi pressure to saturate the sample evenly and squeeze out the excess solution. A picture of using the Mathis HVF model padding machine is shown in Figure 3.12.

Figure 3.12 (Top) Mathis HVF Model Padding Machine and (Bottom) Feeding a Sample into the Padding Machine

Since too high temperature would destroy the pretreatment chemical before printing, the samples were hung on a long hanger after pretreatment in a ventilated pilot laboratory and left out to air dry for forty-eight hours. Wrinkles were created during the pretreating process, and the each sample was ironed from the back after the samples are dried thoroughly.

3.4.3.2 Digital File Preparation

A digital printing file (Figure 3.13) of 29” width and 18” height was created in Adobe Illustrator and saved as tiff file in RGB mode. The file contained seven vertical stripes of cyan (R: 0, G: 255, B: 255), magenta (R: 255, G: 0, B: 255), yellow (R: 255, G: 255, B: 0), black (R: 0, G: 0, B: 0) , red (R: 255, G: 0, B: 0), green (R: 0, G: 255, B: 0), blue (R: 0, G: 0, B: 255), and orange (R: 255, G: 165, B: 0) solid color with 150 ppi resolution.

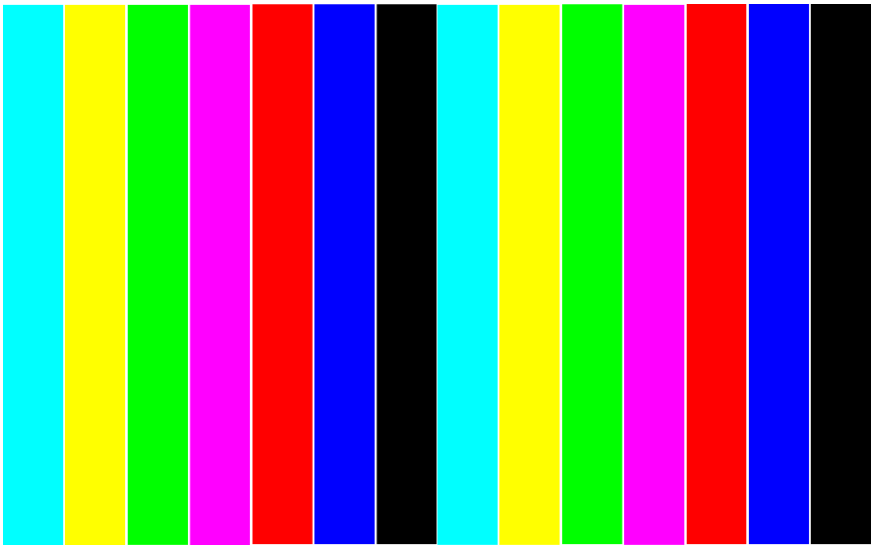

Figure 3.13 A digital file of seven-colored stripes to print

3.4.3.3 Inkjet Printing

Before printing, two laser engraved samples and a sample with no laser treatment were attached to a 63" width roll of fabric with double-sided tape to feed into the roll to roll printer. The dimension of each sample was 37” width and 22” height, and all three samples were located in the middle of the 63” fabric in a row.

A Mutoh ValueJet 1938TX 75” width roll to roll printer (Figure 3.14) with reactive dye was used to apply digital printing on the laser engraved cotton velvet samples (Figure 3.15). The technical specifications of the printer are given in Table 3.3.

Figure 3.14 Mutoh ValueJet VJ-1938TX Printer ("ValueJet 1938TX", n.d.)

Table 3.3 Technical Specifications of Mutoh ValueJet VJ-1938TX (ValueJet 1938TX, n.d.)

Print Technology	Drop-on-demand Micro Piezo Inkjet Technology
Print Heads	2 (staggered setup)
Nozzle Configuration	180 nozzles x 8 lines / head
Drop Mass Range (pl)	3.3 to 45.3
Head Heights	Low: 2.5 mm / Middle: 3.5 mm* / High: 6.0 mm
Max. Print Width	1900 mm (74,80”)
Max. Media Thickness	1.3 / 2.3 / 3.5 mm per head height
Ink Color	Cyan, Magenta, Yellow, Black, Gray, Blue, Red, Orange

*Middle head height was used for sample printing

With RIP Master software, aligning the location of the file within the laser engraved region was achieved by adjusting the x-axis value. Printed samples were located on a clear table in a ventilated room for twenty-four hours to dry naturally.

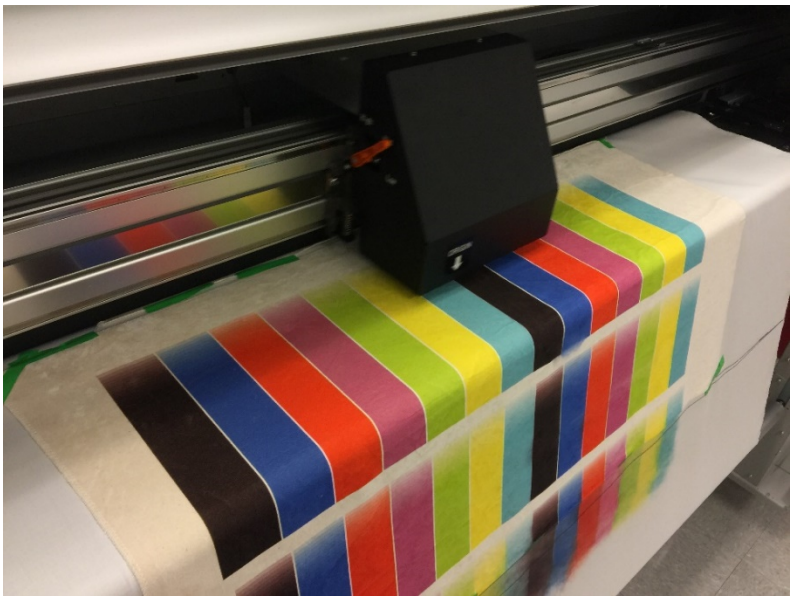

Figure 3.15 Image of a Controlled Velvet Fabric Sample during Printing

3.4.3.4 Posttreatment

In the steaming stage, air and moisture increase gaps between the fibers to help the dye molecules penetrate further into the fabric, and this heat also encourages the development of molecular bonds for maximum color saturation (Cie, 2015).

The printed fabrics were steamed in a Shima Seiki SSM 100 Steamer (Figure 3.16). Each sample was located onto one of the flatbed shelves, and steaming occurred for fifteen minutes at 97 degrees Celcius. An image of the printed samples before and after steaming is shown in Figure 3.17. The color of the printed samples became brighter and more saturated after steaming. Once steaming was completed, the samples were allowed to air dry at room temperature for twenty-four hours before washing.

Figure 3.16 Flatbed Shima Seiki SSM 100 Steam Chamber

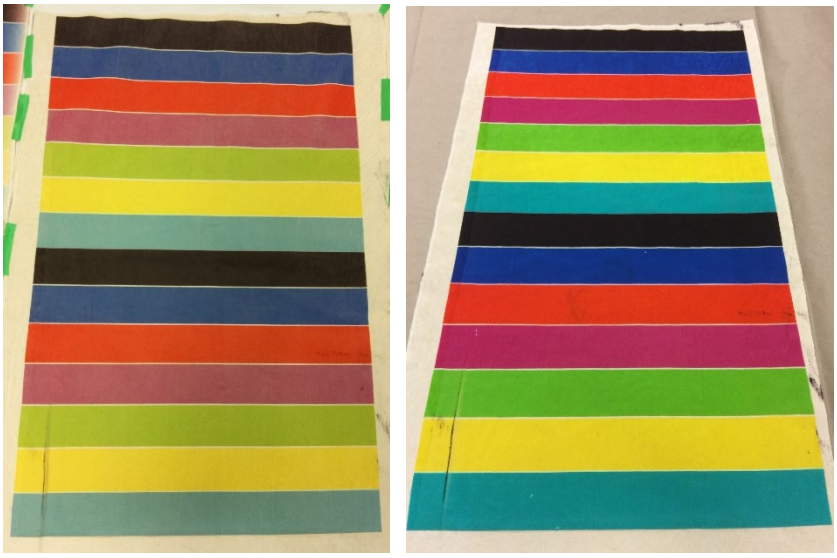

Figure 3.17 (Left) A Printed Sample after Printing and (Right) after Steaming

In the washing stage, the unfixed dye is removed after the steaming process. The amount of printed ink is much greater than required for coloration and the toxic additives in inks must be removed (Cie, 2015; Hawkyard, 2006). After the fabrics were dried, the printed samples were separated into strips by ink color (Figure 3.18), and each strip was washed off separately to keep the ink color from being discolored by the washed-out dye in the water.

Figure 3.18 Slashed Seven Velvet Strips by Ink Color before Washing

The samples were washed with an ATLAS LEF Launder-Ometer (Figure 3.19), which is a washing instrument for colorfastness testing approved by the AATCC (American Association of Textile Chemists and Colorists). The machine maintains constant agitation and precise temperature for reliable test results.

Figure 3.19 ATLAS LEF Launder-Ometer Washing Instrument

Twenty-eight strips (four strips per one color) were distributed into fourteen containers, and each container embodied two strips of one ink color with a 150 mL cleaning solution (Figure

3.20). The cleaning solution was prepared by mixing 3L water and 0.15% AATCC standard detergent.

Figure 3.20 Containers with the cleaning solution

After placing the samples with the cleaning solution into the containers, the containers were covered with a cap and loaded on a stainless steel rotor, which holds the containers and rotates at a constant speed within the instrument (Figure 3.21). The washing machine was operated for forty-five minutes at twenty point nine Celsius (20.9°C).

Figure 3.21 Press-in-place loading for containers on a stainless steel rotor in the Launder-Ometer

After running the Launder-Ometer, all containers were taken out of the machine, and strips were rinsed twice under running water. The washed samples were air-dried in room temperature conditions for forty-eight hours.

Images of magenta, green, and blue color samples before and after washing are shown in Figure 3.22. Considerable color loss was observed after the washing process owing to improper fixation of the dyestuff on the fabric surface or improper removal of unfixed dye. Optimizing the settings and conditions for pretreatment, ink drop size, and posttreatment would be needed to improve poor colorfastness to washing.

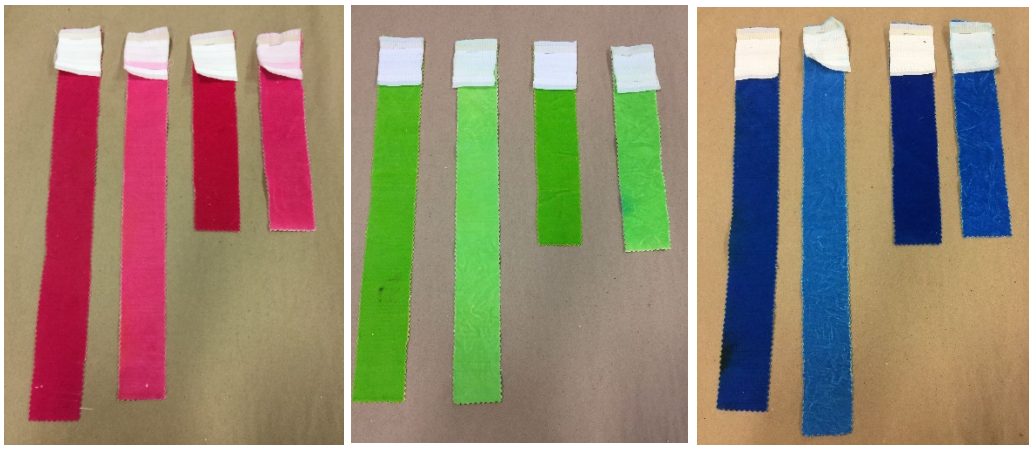

Figure 3.22 Printed color samples before and after washing

3.4.4 Research Stage 3: Colorimetric properties measurement

After the digital textile printing stage, the color properties of the two samples, which contained four different pile depth regions were compared with that of the original velvet fabric material without laser treatment. The colorimetric properties of each sample were measured with a Datacolor 800 spectrophotometer (Figure 3.24 and Table 3.4) using parameters of D65 illuminant with a large aperture (30mm illuminated, 26mm measured) and 10° standard observer functions within the visible spectrum (λ = 400–700 nm). UV and specular light were included, and an average of four readings was obtained.

Figure 3.23 Image of Datacolor 800 spectrophotometer (Left), and Datacolor Tools (Right)

Table 3.4 Technical Specifications of Datacolor 800 spectrophotometer

Instrument type	Dual-beam d/8° spectrophotometer
Illumination source	Pulsed xenon filtered to approximate D65
Sphere diameter	152mm/6 in
Wavelength range	360 nm -700 nm
Wavelength resolution	2 nm
Reporting interval	10 nm
Photometric range	0-200%
Spectral Analyzer	SP2000 analyzer with dual 256 element diode array

Datacolor Tools, which is a color quality application interlocking with the spectrophotometer, allows users to process, manage, extract, and visualize colorimetric data, formulas, and standards. Reflectance curves, CIE L*a*b*, C* and K/S values were obtained from the application. Results were analyzed and interpreted to compare the colorimetric properties of the treated substrates based on laser intensity for different hues.

CHAPTER 4: RESULTS

4.1 Pile Height

A Nikon SMZ 1000 microscope (Figure 4.1) was utilized to measure the pile height. The option of zoom=2 was chosen. Each sample was located under the object lens, and the fine focus was adjusted. NIS-Elements F 4.00.06 software connected with the camera of the microscope provided capture, process, and save images functions. After images were obtained from the microscope, pile heights were measured using ImageJ software.

Figure 4.1 Nikon SMZ 1000 microscope

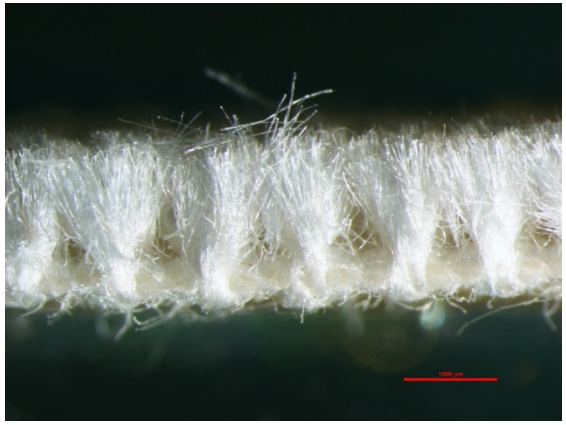

(a) Control

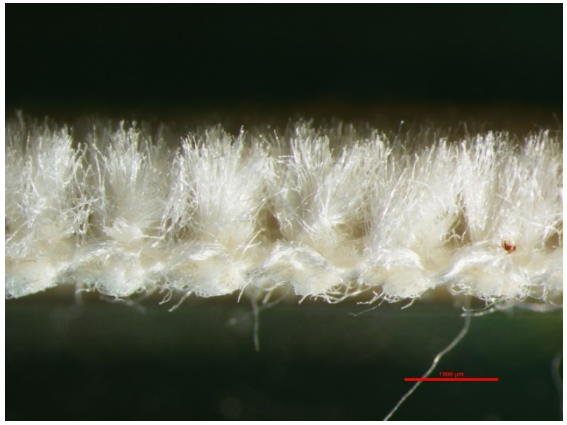

(b) 25% Laser Intensity

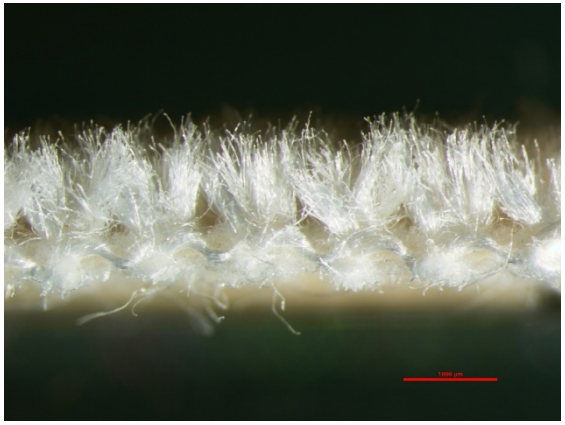

(c) 50% Laser Intensity

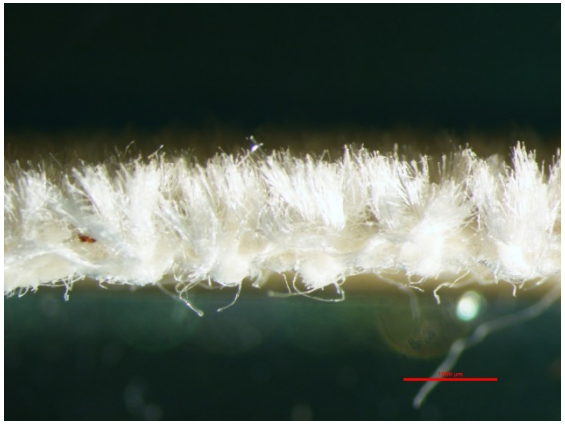

(d) 75% Laser Intensity

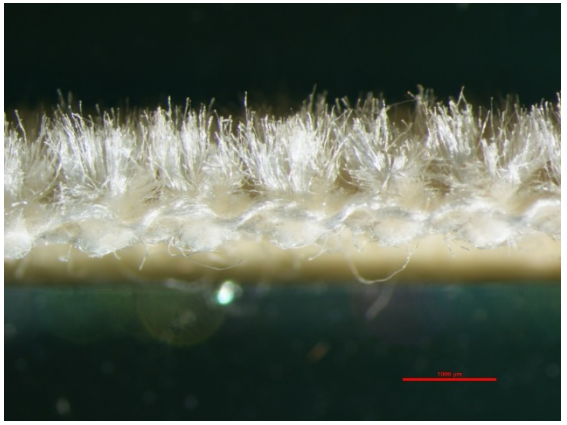

(e) 100% Laser Intensity

Figure 4.2 Micrographs of laser engraved velvet fabric samples: (a) Control, (b) 25%, (c) 50%, (d) 75%, and (e) 100%

Figure 4.2 shows that the pile height of velvet fabric gets shorter as laser intensity increases. For each sample of laser engraved fabric, pile height was measured at several points, and the values were averaged into mean pile height. The average pile height values are listed in Table 4.1. Table 4.1 suggests that the length difference between samples of laser intensity variation is slight compared to the difference between the control sample and laser engraved samples.

Table 4.1 Pile Heights of Velvet Fabrics

Laser Intensity	*Control*	*25%*	*50%*	*75%*	*100%*
Pile Height (μm)	1581.395	1018.605	956.454	891.641	750.388
	1646.512	1137.984	1026.439	1000.000	793.798
	1609.302	1094.574	961.120	969.040	876.744
	1627.907	1102.326	923.795	922.601	933.333
	1679.070	1153.488	956.454	884.675	795.349
		1125.581	1003.110	1026.316	939.535
		1065.116	1013.997	804.954	815.504
			979.782	910.217	776.744
Mean Pile Height (μm)	1628.8 ± 37.0	1099.7 ± 46.2	977.6 ± 34.7	926.2 ± 70.9	835.2 ± 72.3

Micrographs of the printed magenta color inkjet printed on the control and 100% grayscale laser engraved sample are shown in Figure 4.3. The images indicate that the printed magenta color has not penetrated the fabric foundation. Instead, the color ink remained on the surface and imparted colors only to the tip of each fiber.

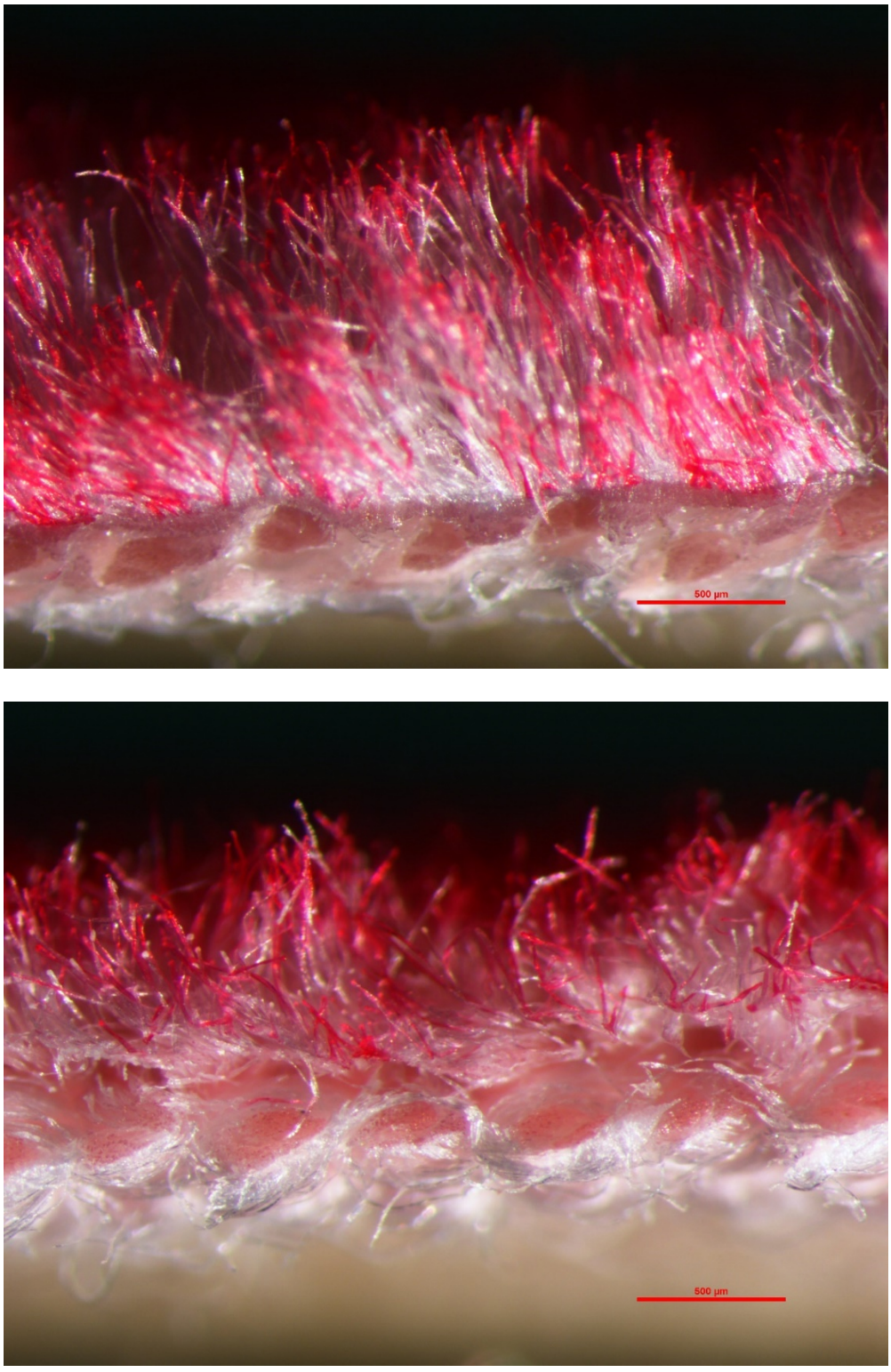

Figure 4.3 (Top) Micrographs of magenta color inkjet printed on the control, and (Bottom) 100% grayscale laser engraved samples

4.2 Spectral Reflectance Curves

Reflectance values represent the percentage of the amount of light leaving a surface divided by the amount of light that strikes it (Johnsen, 2016). The reflectance curve provides information on the depth of shade of the material in the visible spectrum. When the reflectance value is high, the depth of the shade is normally low, and vice versa (Kan, Yuen, & Cheng, 2010; Venkatraman & Liauw, 2019).

For fabrics printed with magenta, yellow, red, and green colors, the reflectance values decreased when the laser treatment was applied. As the surface area available for the coloration of fiber increases, the appearance of the colored fiber would become lighter for a given amount of colorant employed. This could be due to the increased scattering of light from larger surfaces. Moreover, in the case of non-uniformly colored pile, as with inkjet printed pile surfaces, the total amount of reflected light is the sum of light reflected from the white sections and that from the colored tips. The larger the white section, the lighter the appearance of the material. A reduction of pile length can result in a reduction of the sum of reflected light due to reduced scattering and increased absorption of light. However, printed fabrics with black, blue, and cyan colors showed increased reflectance after laser treatments.

The reflectance curves of cyan, magenta, yellow, black, red, green, and blue color are shown in Figures 4.4-4.6, for laser engraved velvet fabric with laser intensity variance of 0%, 25%, 50%, 75%, and 100%. All the samples were inkjet printed after laser engraving.

4.2.1 Printed Color: Cyan, Green, and Blue

Figure 4.4 depicts reflectance curves of cotton velvet fabric printed with cyan, green, and blue color respectively on laser engraved substrates of control, 25%, 50%, 75%, and 100% laser intensity.

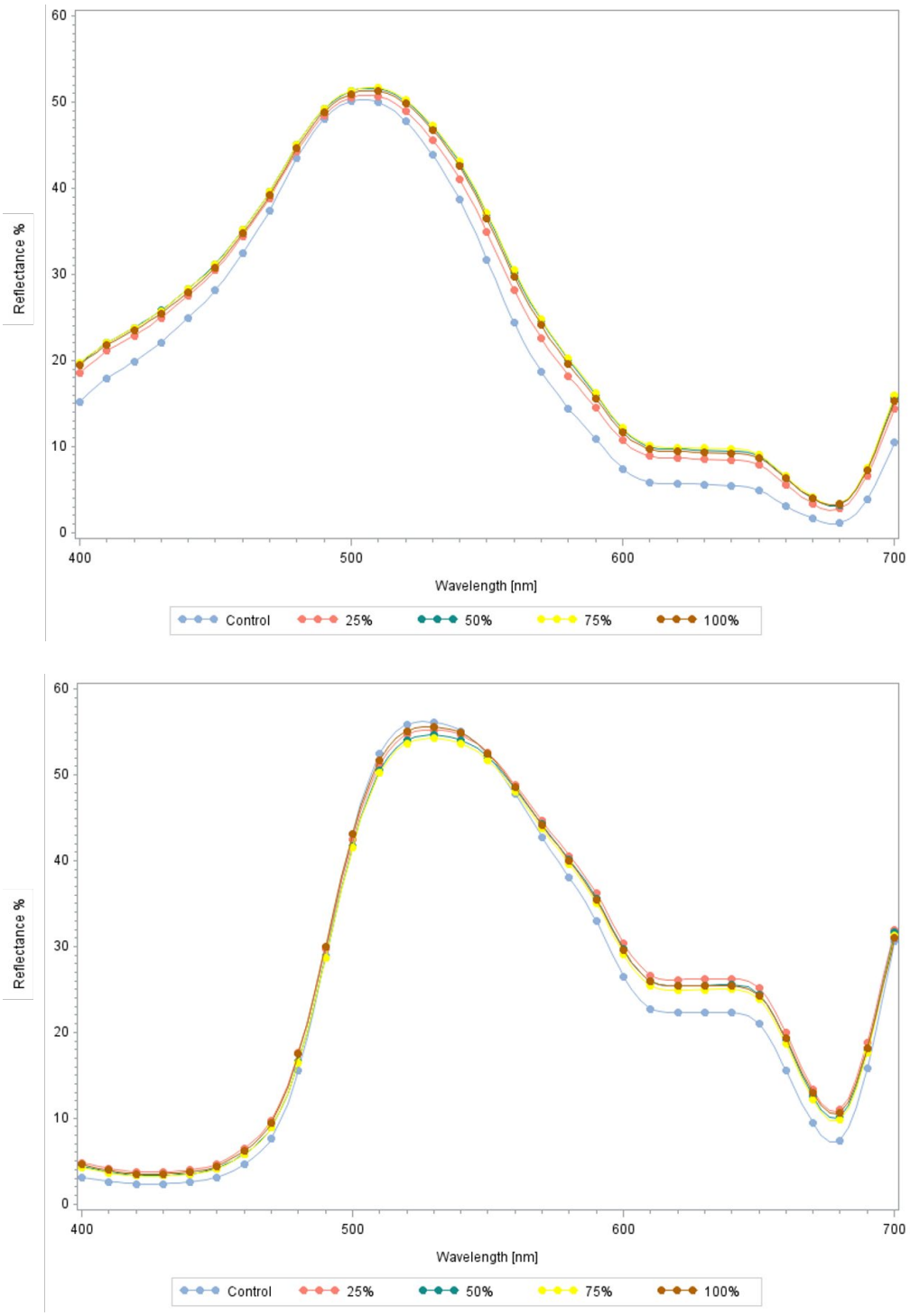

Figure 4.4 Reflectance Curves of Cotton Velvet Fabrics Printed with a (Top) Cyan, (Middle) Green, and (Bottom) Blue Printed on Laser Engraved Substrates

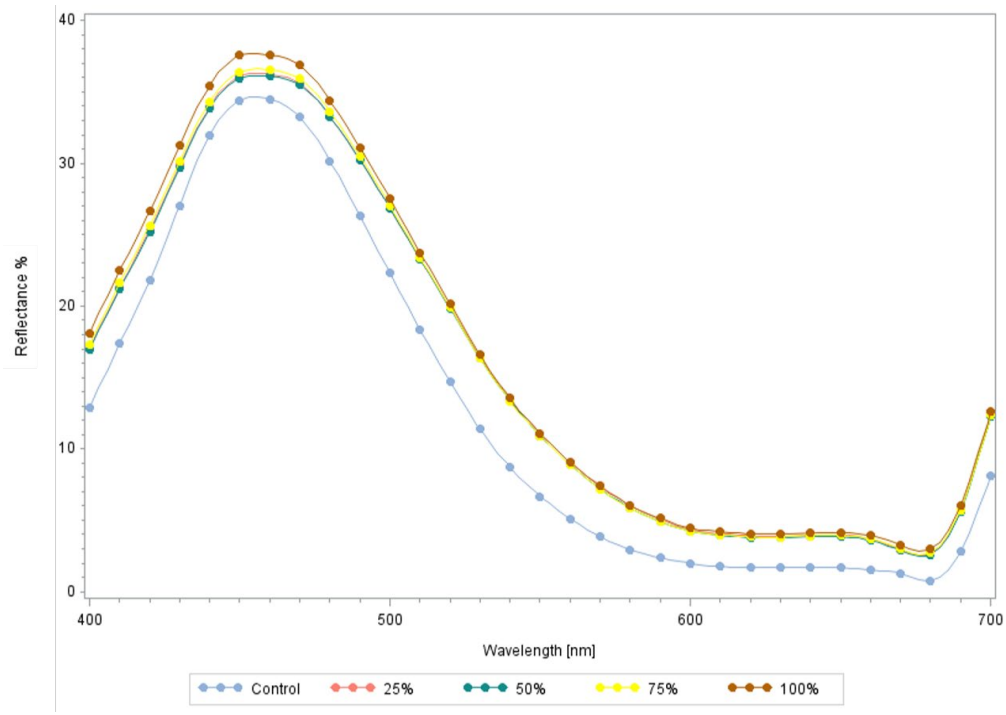

Figure 4.4 Reflectance Curves of Cotton Velvet Fabrics Printed with a (Top) Cyan, (Middle) Green, and (Bottom) Blue Printed on Laser Engraved Substrates continued

For cyan and blue printed colors, across the spectrum, the reflectance value decreases, and absorption increases as laser intensity is reduced. In other words, samples with longer pile heights show lower reflectance value, and a deeper bluish surface appearance than the laser engraved samples. The control fabric printed with green has the highest reflectance values between 500 nm to 540 nm (corresponding to its green color) and the lowest reflectance values in the rest of the spectrum. However, the reflectance value does not change consistently with laser intensity order.

4.2.2 Printed Color: Red, Yellow, and Magenta

Figure 4.5 depicts reflectance curves of cotton velvet fabric printed with red, yellow, and magenta colors respectively on laser engraved substrates treated with 25%, 50%, 75%, and 100% laser intensity as well as the untreated control.

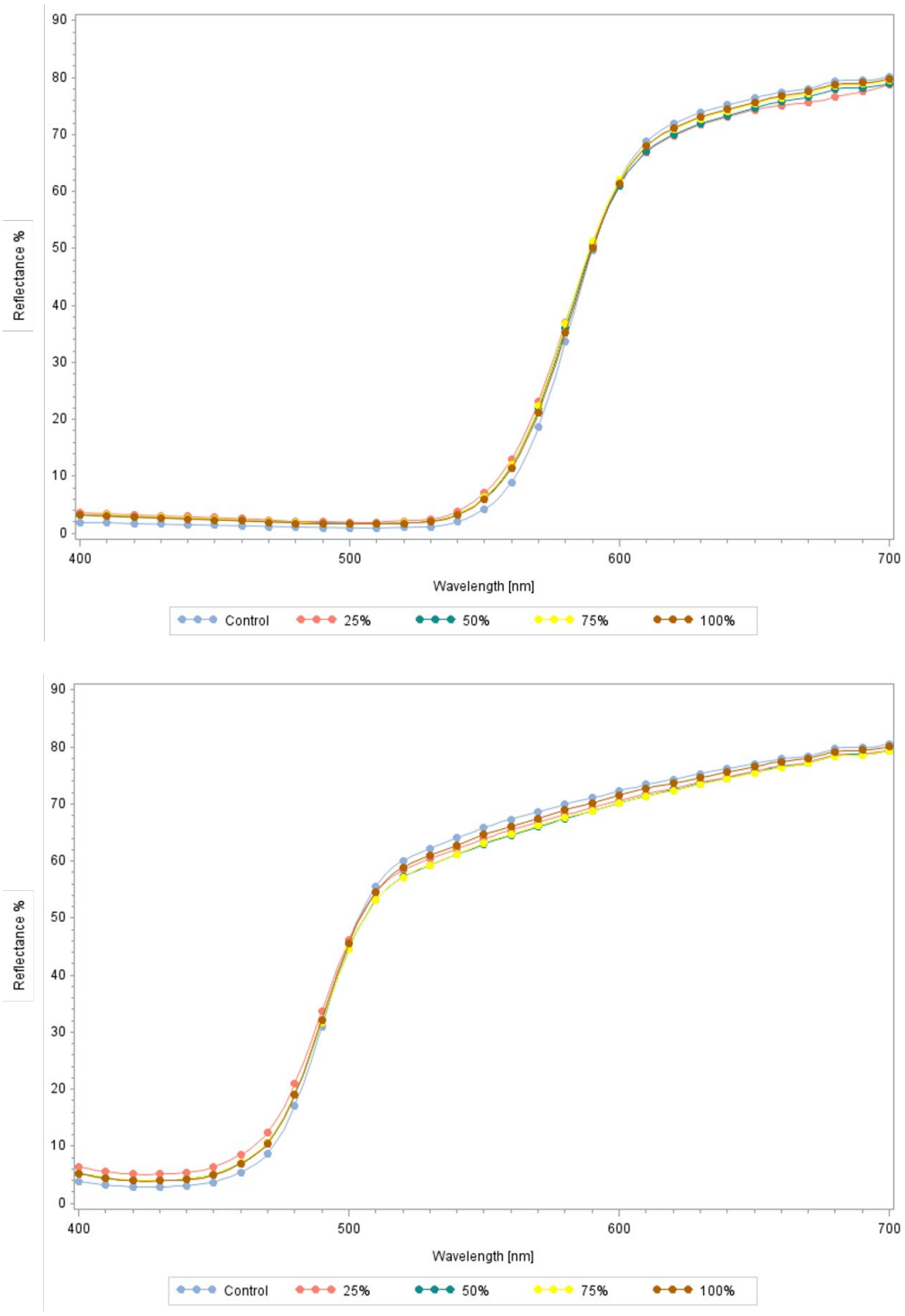

Figure 4.5 Reflectance Curves of Cotton Velvet Fabrics Printed with a (Top) Red, (Middle) Yellow, and (Bottom) Magenta Printed on Laser Engraved Substrates

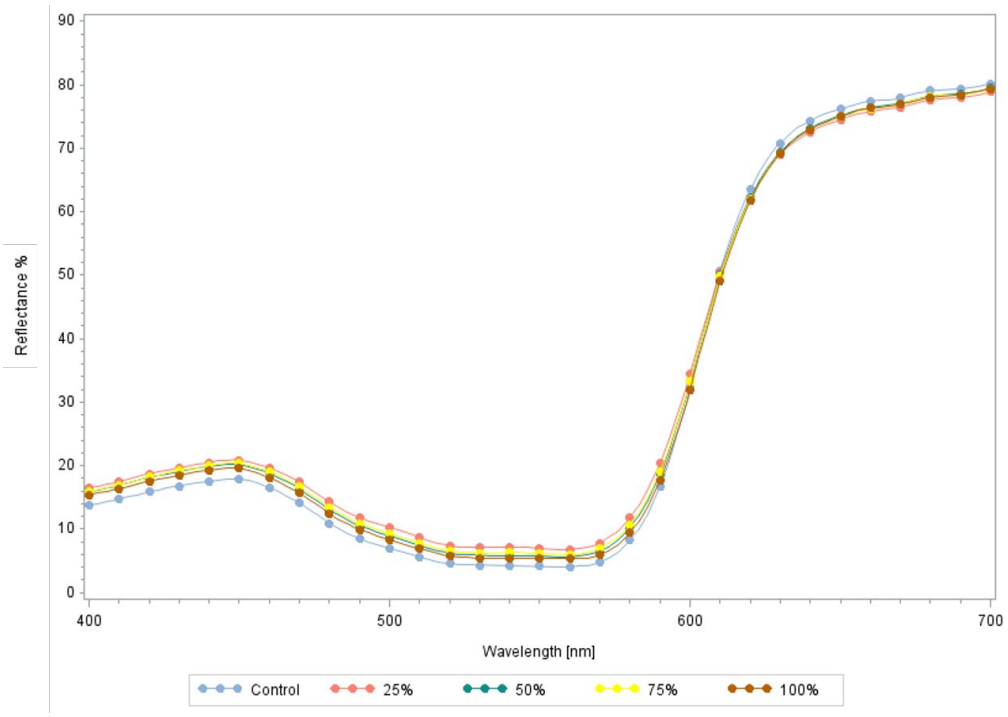

Figure 4.5 Reflectance Curves of Cotton Velvet Fabrics Printed with a (Top) Red, (Middle) Yellow, and (Bottom) Magenta Printed on Laser Engraved Substrates continued

All reflectance curves have the highest peak values around 500 nm to 700 nm. The control fabric, however, has the highest reflectance value. This means that the sample with the longest pile height and the largest surface area should appear lighter than the laser engraved samples. Nevertheless, laser engraved fabrics at four different intensities reveal an inconsistent pattern in relation to reflectance values.

4.2.3 Printed Color: Black

Figure 4.6 depicts the reflectance curves of cotton velvet fabric printed with black on laser engraved substrates treated with 25%, 50%, 75%, and 100% laser intensities and the untreated control.

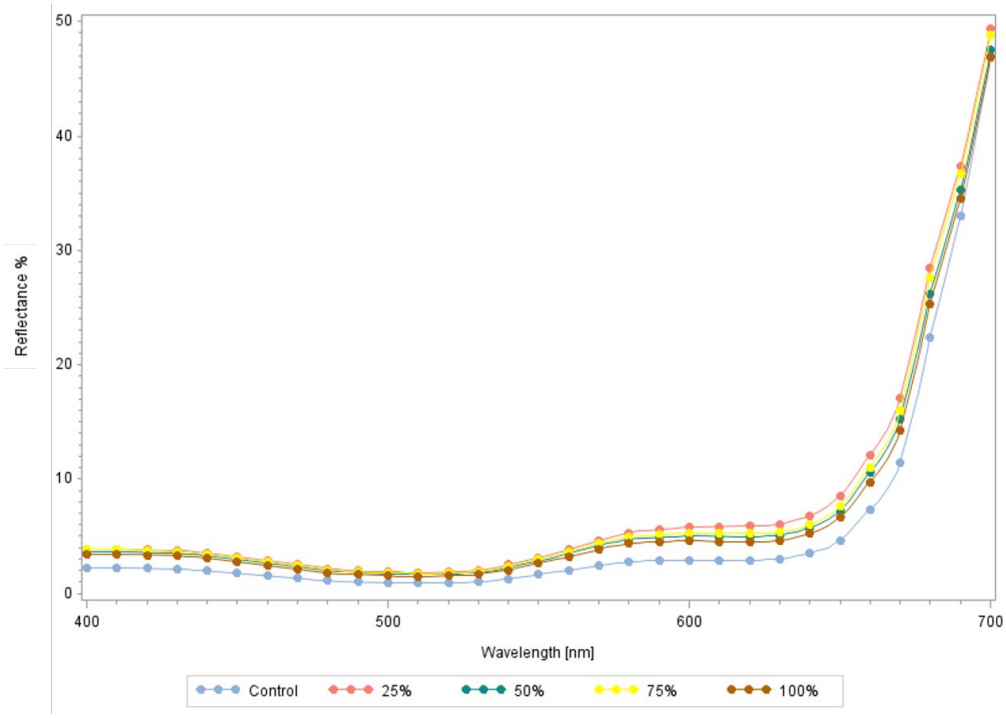

Figure 4.6 Reflectance Curves of Cotton Velvet Fabrics Printed with Black Printed on Laser Engraved Substrates

Across the visible spectrum, the control sample has the lowest reflectance value. The longest pile height exhibited the deepest/darkest blackish surface appearance compared to the other laser engraved samples.

Over 95% of the incident light is absorbed between 400 nm to 650 nm, but the black sample shows a peak at around 700 nm, i.e., the red region, implying a reddish-black appearance. The black color was not premixed but mixed as required from combinations of cyan, magenta, yellow, black, gray, blue, red, and orange inks used on the printing machine. After the washing process, a considerable degree of color loss was observed, and the printed black color became brownish in appearance.

4.3 Colorimetric, Color Strength and Color Difference Values

Table 4.2 demonstrates the difference in L*, a*, b*, C*, $\Delta E_{cmc,}$ and K/S_{sum} values between control and four laser engraved (25%, 50%, 75%, and 100% intensity) cotton velvet fabrics.

Table 4.2 Colorimetric and Color Strength Values for Printed Colors on Velvet Fabrics

Color	***Laser Intensity***	***L****	***a****	***b****	***C****	ΔE_{cmc}	K/S_{sum}
Cyan	Control	60.37	-50.01	-2.81	50.09		175.5
	25%	62.58	-44.08	-2.05	44.13	2.51	94.61
	50%	63.79	-42.90	-1.04	42.91	3.23	82.49
	75%	63.92	-42.77	-0.78	42.78	3.33	80.12
	100%	63.48	-43.30	-1.08	43.31	3.04	83.46
Magenta	Control	45.41	58.91	-1.56	58.93		112.95
	25%	48.72	51.88	-2.53	51.95	3.06	70.81
	50%	47.3	54.73	-3.23	54.83	2	83.67
	75%	47.7	53.71	-2.98	53.79	2.33	79.29
	100%	46.55	55.5	-3.26	55.59	1.64	90.26
Yellow	Control	82.11	-5.19	82.96	83.12		104.03
	25%	81.5	-4.65	73.27	73.41	3.07	59.71
	50%	80.99	-4.18	76.67	76.78	2.06	76.11
	75%	81.02	-4.22	76.62	76.74	2.07	75.65
	100%	81.72	-4.62	77.99	78.12	1.59	76.84

Table 4.2 Colorimetric and Color Strength Values for Printed Colors on Velvet Fabrics continued

Color	*Laser Intensity*	*L**	*a**	*b**	*C**	ΔE_{cmc}	K/S_{sum}
	Control	15.38	14.59	2.62	14.83		747.99
	25%	22.96	16.75	4.39	17.32	7.74	379.26
Black	50%	21.46	15.61	3.32	15.96	6.03	420.8
	75%	22.04	15.86	3.42	16.22	6.61	401.18
	100%	20.4	15.37	3.12	15.69	4.96	463.39
	Control	52.18	61.01	69.72	92.65		597.5
	25%	53.87	56.58	60.2	82.61	3.9	287.62
Red	50%	53.33	57.71	62.02	84.72	3.19	336.14
	75%	53.66	57.97	62.28	85.08	3.14	331.12
	100%	53.23	58.42	62.37	85.46	3.17	345.75
	Control	69.74	-40.26	64.98	76.44		153.31
	25%	70.57	-34.72	60.83	70.04	2.41	99.99
Green	50%	70.15	-35.03	62.18	71.37	2.15	111.32
	75%	69.88	-35.4	61.96	71.36	2.03	113.77
	100%	70.46	-36.03	61.32	71.12	1.92	105.63
	Control	37.74	-10.07	-41.92	43.11		414.91
	25%	43.8	-13.87	-34.99	37.64	5.43	174.42
Blue	50%	43.64	-14.16	-35.11	37.86	5.45	179.11
	75%	43.72	-13.81	-35.56	38.15	5.21	175.75
	100%	44.14	-13.09	-36.21	38.5	4.91	165.59

As a rank-based nonparametric alternative to the one-way ANOVA with repeated measures, the Friedman test is utilized to test for differences between dependent groups when an outcome variable is ordinal or continuous data that hasn't fulfilled the assumptions required in parametric tests (e.g., normality, homogeneity of variances) or when there is no way to test the assumptions because of a small sample size (Conover & Conover, 1999; Dwivedi et al., 2017; Friedman, 1940). The process includes ranking each row (or block) together and then taking the values of ranks by columns into account (National Institute of Standards and Technology, 2015). In this case, samples were sorted by printed color (block) and ranked in the analysis.

In this work, a Friedman test was used to understand whether the six color properties (L*, a*, b*, C*, ΔE_{cmc}, K/S_{sum}) measured on a continuous scale, differed based on the five laser treatment conditions (Control, 25%, 50%, 75%, 100%) and the seven printed colors (Cyan, Magenta, Yellow, Black, Red, Green, Blue). In this experimental design, all of the printed velvet samples were measured. In the analysis, each color group included the data for all laser treatment conditions. The five laser treatment conditions were regarded as repeated measures on the same dependent variables.

According to previous studies (e.g., Bae, et al., 2015; Ding et al., 2019; Lim & Chapman, 2019; Pourdeyhimi, 1994), the object color influences the L*, a*, b*, C*, ΔE, and K/S values of a non-self-luminous surface. Therefore, the printed color effect should be controlled when looking at the effect of laser intensity on the color properties of the printed colors. By sorting according to printed color in the analysis, the predictor that triggers the variability between the samples can be controlled. As a result, just the variability within the subjects is involved in the error term, which in turn minimizes residuals and enhances the power of the analysis (The Minitab Blog Editor, 2015).

Table 4.3 An example of the Friedman test: using L* data

Blocks (Printed Colors)	Treatments (Intensity Levels)									
	Control		25%		50%		75%		100%	
	x	r (rank)	x	r (rank)	x	r (rank)	x	r (rank)	x	r (rank)
Cyan	60.37	1.00	62.58	2.00	63.79	4.00	63.92	5.00	63.48	3.00
Magenta	45.41	1.00	48.72	5.00	47.3	3.00	47.7	4.00	46.55	2.00
Yellow	82.11	5.00	81.5	3.00	80.99	1.00	81.02	2.00	81.72	4.00
Black	15.38	1.00	22.96	5.00	21.46	3.00	22.04	4.00	20.4	2.00
Red	52.18	1.00	53.87	5.00	53.33	3.00	53.66	4.00	53.23	2.00
Green	69.74	1.00	70.57	5.00	70.15	3.00	69.88	2.00	70.46	4.00
Blue	37.74	1.00	43.8	4.00	43.64	2.00	43.72	3.00	44.14	5.00
$\bar{r}_j$	$\bar{r}_{.1} = 1.57$		$\bar{r}_{.2} = 4.14$		$\bar{r}_{.3} = 2.71$		$\bar{r}_{.4} = 3.43$		$\bar{r}_{.5} = 3.14$	

*4.3.1 CIE L**

CIE L* value defines the lightness of the measured samples. The higher the L* value, the lighter the sample color will be, and the lower the L* value, the darker the color of the sample will be (Berns, 2019).

A Friedman test showed that there was a statistically significant difference in the L* mean ranks between the different laser treatment conditions, $\chi^2(4) = 10.171, p = 0.038$. The L* mean rank scores were 1.57 for the untreated control, and 4.14, 2.71, 3.43, and 3.14 for treatment conditions 25%, 50%, 75%, and 100% respectively.

Table 4.4 Friedman Test Result of L* by Intensity

L* Mean Rank by Intensity					Friedman Test Statistics			
Control	25%	50%	75%	100%	N	χ^2	df.	Sig.
1.57	4.14	2.71	3.43	3.14	7	10.171	4	.038*

Note: * $p < .05$, ** $p < .01$, *** $p < .001$.

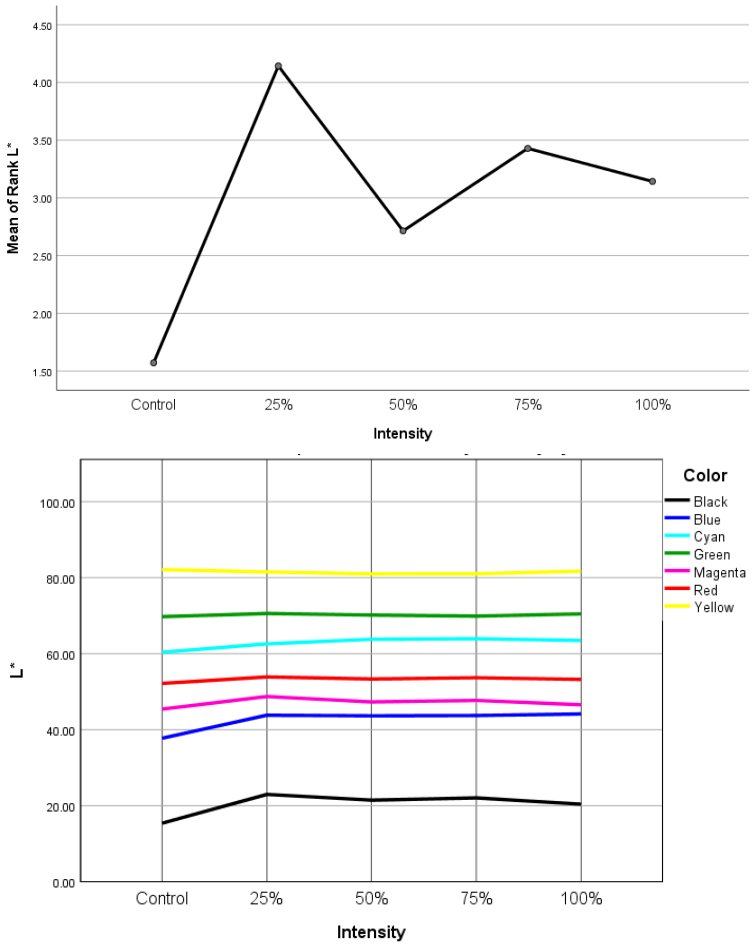

Figure 4.7 (Top) L* Mean Rank for All Colors by Intensity and (Bottom) L* Value by Intensity

The L* mean rank slightly increased, and the shade became lighter when the laser treatment was applied, for almost all printed colors except yellow. The yellow sample exhibited the opposite result: i.e. a reduction in the L* value which led to a darker shade of color with laser treatment. However, four laser engraved samples with intensity variation reveal an inconsistent order of L* value. The order of L* value by the printed color from the highest to the lowest is yellow, green, cyan, red, magenta, blue, and black regardless of laser intensity.

*4.3.2 CIE a**

CIE a* value indicates the redness and greenness of a sample. Larger positive a* values, indicate redder shades of the sample; and larger negative a* values, imply greener samples.

A Friedman test showed that there was not a statistically significant difference in a* mean ranks for the different laser treatment conditions, $\chi^2(4) = 1.371, p = 0.849$. The a* mean rank scores were of 2.71 for the untreated control, and 2.57, 3.14, 3.43, and 3.14 for treatment conditions 25%, 50%, 75%, and 100% respectively.

Table 4.5 Friedman Test Result of a* by Intensity

a* Mean Rank by Intensity					Friedman Test Statistics			
Control	25%	50%	75%	100%	N	χ^2	df.	Sig.
2.71	2.57	3.14	3.43	3.14	7	1.371	4	.849

Note: * $p < .05$, ** $p < .01$, *** $p < .001$.

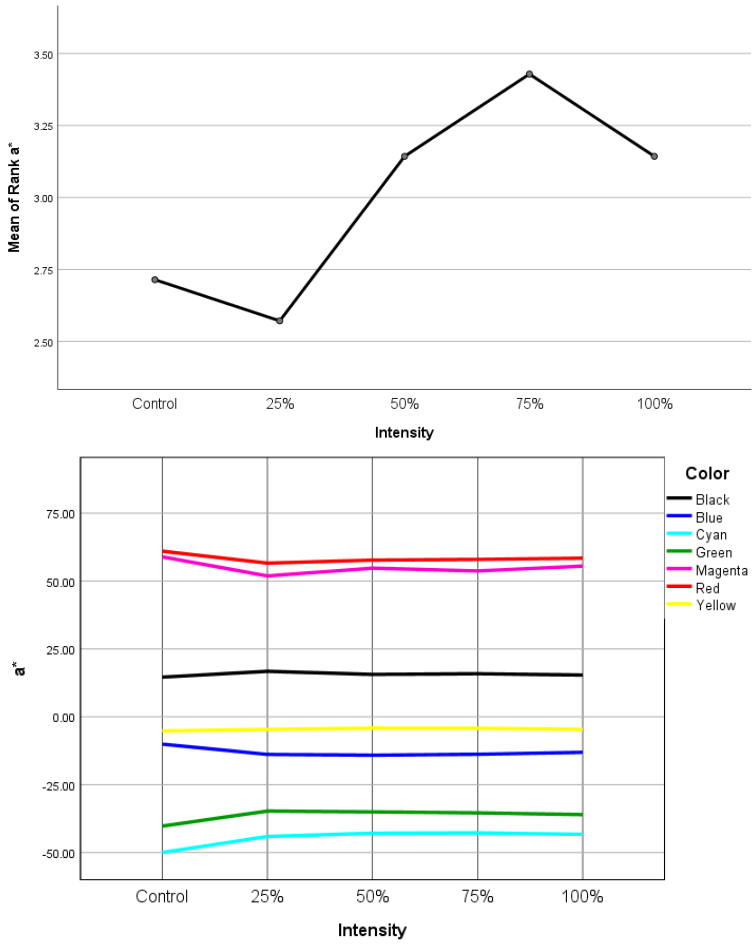

Figure 4.8 (Top) a* Mean Rank for All Colors by Intensity and (Bottom) a* Value by Intensity

Comparing the control, to the 25% laser intensity sample, it is notable that the a* mean rank slightly increased for the treated samples. The black, yellow, green, and cyan printed colors became redder, whereas red, magenta, and blue printed colors became greener (Figure 4.8).

Yellow, blue, green, and cyan samples have negative a* values across all samples regardless of laser intensity variation. The samples printed with yellow, green, and cyan became less green with laser treatment. However, the blue printed sample became greener. Green and cyan exhibit the greatest gaps between the highest and the lowest a* values among these four colors.

Red, magenta, and black samples have positive a* values across all samples regardless of laser intensity variation. The magenta and red samples became less red with laser treatment. However, the black samples became redder. Black samples have the greatest gaps between the highest and the lowest a* values among these three colors.

*4.3.3 CIE b**

The b* value describes the yellowness and blueness of a sample. The more positive b* value, the yellower the shade of the sample; the more negative b* value, the bluer the sample's shade.

A Friedman test showed that there was not a statistically significant difference in b* mean ranks between the different laser treatment conditions, $\chi^2(4) = 1.257, p = 0.869$. The b* mean rank scores were 3.29 for the untreated control, and 2.71, 3.14, 3.29, and 2.57 for treatment conditions 25%, 50%, 75%, and 100% respectively.

Table 4.6 Friedman Test Result of b* by Intensity

b* Mean Rank by Intensity					Friedman Test Statistics			
Control	25%	50%	75%	100%	N	χ^2	df.	Sig.
3.29	2.71	3.14	3.29	2.57	7	1.257	4	.869

Note: * $p < .05$, ** $p < .01$, *** $p < .001$.

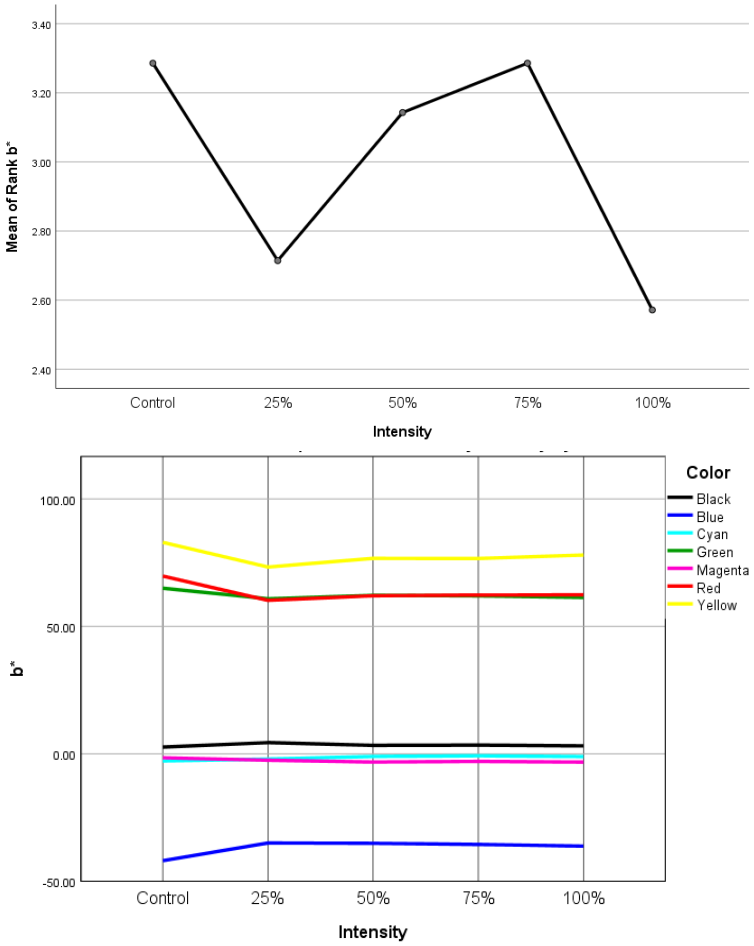

Figure 4.9 (Top) b* Mean Rank for All Colors by Intensity and (Bottom) b* Value by Intensity

The b* mean rank slightly decreased, i.e. colors became bluer, when the laser treatment was applied, especially in yellow, red, green, and magenta printed colors. On the other hand, the black, cyan, and blue printed colors became yellower when laser treatment was applied (Figure 4.9).

Cyan, magenta, and blue samples have negative b* values across all samples regardless of laser intensity variation. The cyan and blue samples became less blue with laser treatment. In contrast, the magenta sample became bluer. Blue sample showed the greatest difference between the highest and the lowest b* value among the three colors that have negative b* values.

Yellow, red, green, and black samples have positive b* values across all samples regardless of laser intensity variation. The yellow, red, and green samples became less yellow when laser treatment was applied. In contrast, the black samples became yellower with laser treatment. Red and yellow samples show the greatest difference between the highest and lowest b* value among the four colors with positive b* value.

*4.3.4 CIE C**

Chroma, C* indicates the purity, colorfulness, or departure from gray for various hues. The value increases for increased amounts of colorants present on a fabric surface. Higher C* is described as more vivid while lower C* is paler (Hunt & Pointer, 2011).

A Friedman test showed that there was a statistically significant difference in C* mean ranks among the different laser treatment conditions, $\chi^2(4) = 9.486, p = 0.05$. The C* mean rank scores were 4.43 for the untreated control, and 2.00, 2.71, 2.57, and 3.29 for treatment conditions 25%, 50%, 75%, and 100% respectively.

Table 4.7 Friedman Test Result of C* by Intensity

C* Mean Rank by Intensity					Friedman Test Statistics			
Control	25%	50%	75%	100%	N	χ^2	df.	Sig.
4.43	2.00	2.71	2.57	3.29	7	9.486	4	.05*

Note: * $p < .05$, ** $p < .01$, *** $p < .001$.

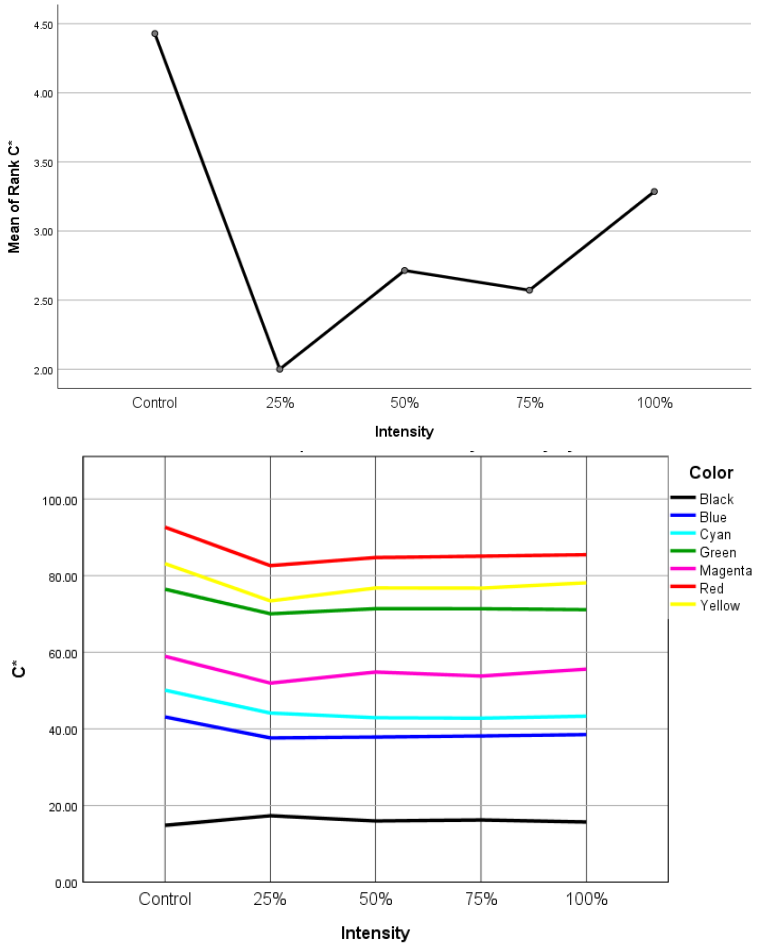

Figure 4.10 (Top) C* Mean Rank for All Colors by Intensity and (Bottom) C* Value by Intensity

Other than for the black printed samples, the C* mean rank decreased when the laser treatment was applied, similar to that for the b* values. The order of C* value for the printed samples from the highest to the lowest is red, yellow, green, magenta, cyan, blue and black regardless of laser intensity. Shorter pile heights exhibited lower color intensity. In other words, this implies decreased amounts of colorants are present on the shorter pile substrate. However, four laser engraved samples with intensity variation indicate an inconsistent correlation against C* value.

4.3.5 K/S$_{sum}$

K/S values are obtained using the Kubelka-Munk function and denote the color yield or color strength of fabrics (Kan, Yuen, & Cheng, 2012; Venkatraman & Liauw, 2019). K is the absorption coefficient of a colorant, and S is the scattering coefficient. As absorption increases, color strength becomes greater (Lim & Chapman, 2019). The sum of the K/S values in the visible region of the color spectrum was calculated.

A Friedman test showed that there was a statistically significant difference in the K/S$_{sum}$ mean ranks between the different laser treatment conditions, $\chi^2(4) = 17.943, p = 0.001$. The K/S$_{sum}$ mean rank scores were 5.00 for the untreated control, and 1.71, 3.14, 2.14, and 3.00 for treatment conditions 25%, 50%, 75%, and 100% respectively.

Table 4.8 Friedman Test Result of K/S$_{sum}$ by Intensity

K/S$_{sum}$ Mean Rank by Intensity					Friedman Test Statistics			
Control	25%	50%	75%	100%	N	χ^2	df.	Sig.
5.00	1.71	3.14	2.14	3.00	7	17.943	4	.001***

Note: * $p < .05$, ** $p < .01$, *** $p < .001$.

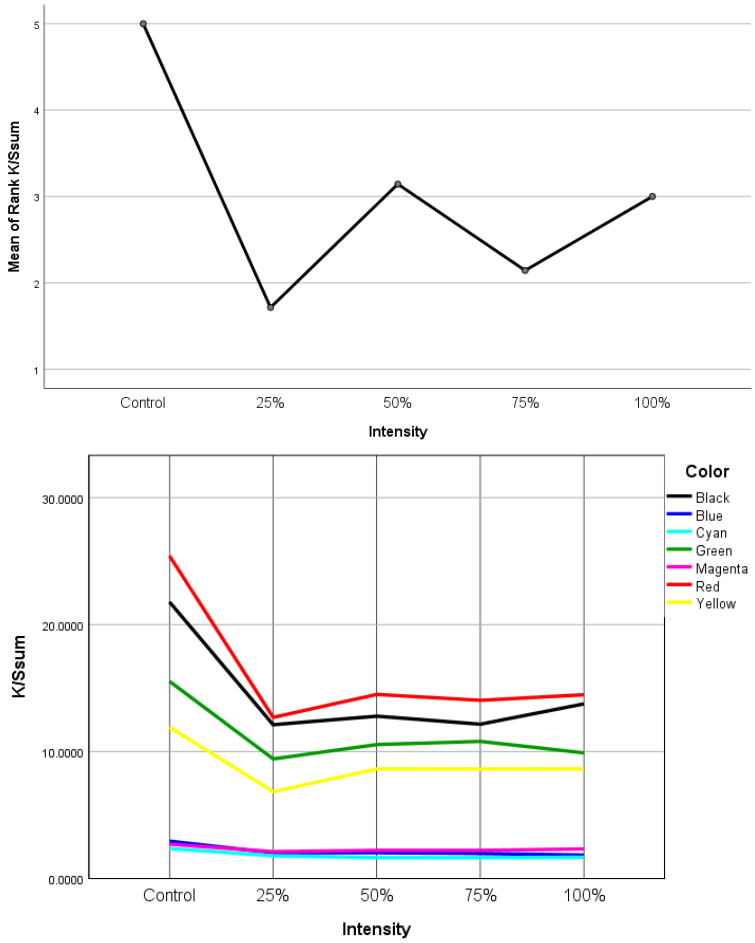

Figure 4.11 (Top) K/S_{sum} Mean Rank for All Colors by Intensity and (Bottom) K/S_{sum} by Intensity

The K/S_{sum} mean rank decreased when the laser treatment was applied, similar to the b*, and C* and in contrast to L* across all colors. This indicates a weaker color strength for the laser engraved samples due to the increased removal of piles from the substrate. The order of the K/S_{sum} values for the printed samples from the highest to the lowest is red, black, green, yellow, magenta, blue, and cyan regardless of the laser intensity. The K/S_{sum} value of blue, magenta, and cyan had a minute fluctuation for all laser intensities. Moreover, the K/S_{sum} values of the four laser engraved samples with intensity variation appear in an inconsistent order.

4.3.6 ΔE_{cmc}

The total color difference, represented by ΔE or DE, is the quantification of the perceptual difference between two colors. It indicates the difference or distance between two given colored stimuli in the CIE L*a*b* color space. The CMC tolerancing method directly addresses our "elliptical" perception of color difference and represents the area of acceptance concerning the standard (X-rite, 2019). The L*a*b* values of the standard (control) were used to calculate the color difference between the original fabric and colors imparted following the laser treatments.

A Friedman test showed that there was a statistically significant difference in the ΔE_{cmc} mean ranks between the different laser treatment conditions, $\chi^2(3) = 10.029, p = 0.018$. The ΔE_{cmc} mean rank scores were 3.43, 2.71, 2.57, and 1.29 for treatment conditions 25%, 50%, 75%, and 100% respectively.

Table 4.9 Friedman Test Result of ΔE_{cmc} by Intensity

ΔE_{cmc} Mean Rank by Intensity					Friedman Test Statistics			
Control	25%	50%	75%	100%	N	χ^2	df.	Sig.
N/A	3.43	2.71	2.57	1.29	7	10.029	3	.018*

Note: * $p < .05$, ** $p < .01$, *** $p < .001$.

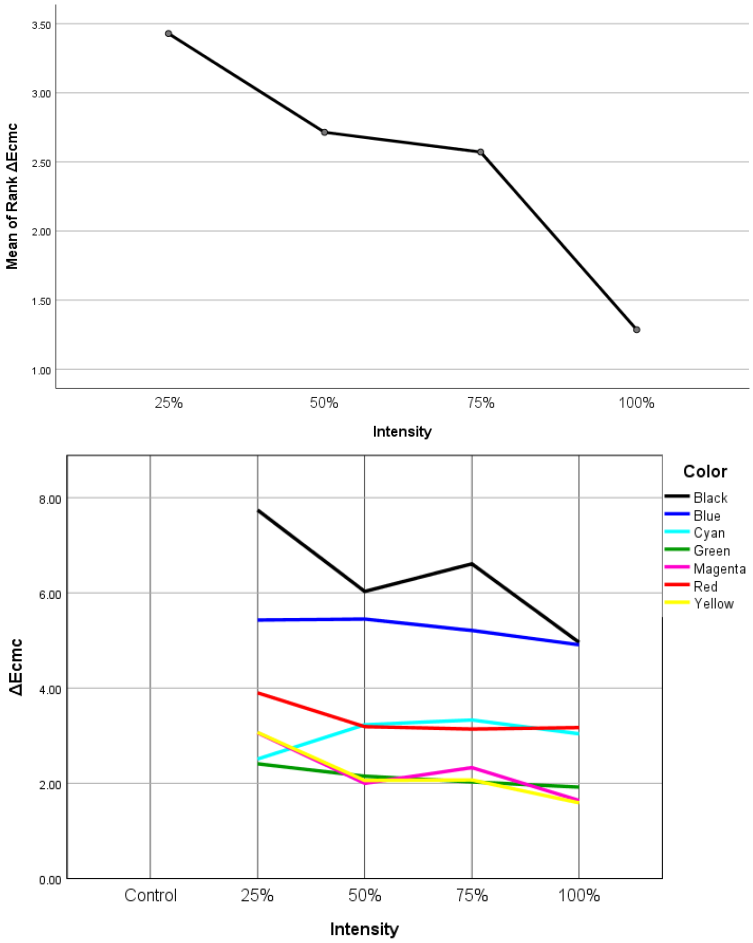

Figure 4.12 (Top) ΔE_{cmc} Mean Rank for All Colors by Intensity and (Bottom) ΔE_{cmc} value by Intensity

For the total color difference, control fabric with no laser treatment was standard for each color. It is interesting that the ΔE_{cmc} mean rank decreased when the laser treatment was applied, similar to the color attributes b*, C*, and K/S_{sum} other than for cyan. Moreover, the increment of laser intensity resulted in the smaller difference of ΔE_{cmc} score between colors.

Across all laser intensity options, black and blue have significantly higher ΔE_{cmc} values compared to other colors. It implies that laser treatment has more impact on color properties of black and blue than for other colors. Moreover, the ΔE_{cmc} value of black has the most significant variation among all printed colors, which means that the relationship between the magnitude of the color difference and pile height was inconsistent.

CHAPTER 5:

DISCUSSION, CONCLUSIONS, AND RECOMMENDATIONS

5.1 Discussion, Conclusions, and Future Research

In this paper, the color attributes of laser engraved and digital printed cotton velvet fabric were examined to assess their color variation effects.

First of all, the results indicate that the cotton velvet fabric treated by the laser can achieve sculpture through partial and controlled removal of portions of fibers, and change surface contour by adjusting laser intensity. The micrographs of laser engraved cotton velvet samples denote that pile height was adjusted by changing laser intensity with a grayscale of graphics under consistent laser power, speed, and pixels per inch.

Next, the experiments revealed that the changes in surface morphology of cotton velvet fabric printed by a digital printer with reactive dye achieved variable reflectance values, lightness, chroma, total color difference, and color strength. The changes in the color properties are mainly related to the surface area available for the coloration of fiber and its appearance. The increased removal of pile fibers after laser treatment reduced the surface available for colorant absorption as well as light loss in these regions.

Laser treatment increased lightness, measured in terms of L*, except in the case of yellow samples. Increased L* values reported in this research agree with the existing literature, which suggests that consistent increases in L*, up to a certain extent, are associated with increased levels of compactness of piles in collapsed carpets (Wood, 1993). Chroma, as measured by C*, decreased when the laser treatment was applied because of reduced dye absorption on the surface of the fabric. A reduction in pile length resulted in a decrease in color strength, as measured by K/S_{sum} would be consistent with the C* reduction for all printed colors. Moreover, the total color

difference measured by ΔE_{cmc} between the controlled sample and laser engraved samples decreased for all printed colors except for cyan by an increase in laser intensity.

Notably, laser engraved samples treated at four laser intensities revealed an inconsistent order of change in their colorimetric attributes and reflectance values. Microscope images and pile height measurement implies that the pile height variation between the laser engraved samples may be too minute to result in meaningful and ordered color differences among samples.

Finally, the results of this study signify that the effect of laser intensity on the colorimetric properties of printed samples may be hue dependent. Laser treatment resulted in lower reflectance values for magenta, red, yellow, and green colored samples. By contrast, printed cyan, blue, and black colors had higher reflectance values when laser treatment was applied. In other words, reduced pile height led to cyan, blue, and black printed colors producing paler shades. In those cases, the removal of the pile resulted in increased reflectance from the white background substrate. In the case of dark colors, the low signal to noise ratios can increase the effect of noise on readings. In the case of color strength, red and black printed colors had the highest, whereas magenta, blue, and cyan exhibited the lowest. The printed black and cyan became redder and yellower, and the printed red and magenta became greener and bluer after laser treatment.

Pourdeyhimi (1994) asserts that there is a physical restriction to the brightness of non-self-luminous surfaces: the highest brightness value relies on the object's hue. In this research, yellow, red, and green printed colors were ranked highest on both mean L*, and C* values out of all printed colors. Furthermore, black and blue had significantly higher ΔE_{cmc} values compared to other colors across all laser treatment conditions. This result supports the finding that darker shades show more extreme color differences as texture difference increases (Bae et al., 2015; Bae, 2008).

This research could be a key step toward developing an integrated laser treatment and digital inkjet printing manufacturing approach for the apparel and textile design industry. Melding the two technologies accomplished various textures and modification of the color properties of the cotton velvet fabric. Instrumental color measurement data can be used to predict the color quality of the substrate, determining settings for specific surface design effects, and for practitioner use in mass customization approaches.

Future work will aim at accumulating optimal setting data of the laser machine and inkjet printer to achieve design requirements for clearer engraving patterns and different shade effects to achieve ideal aesthetic effects for fashion and textile design. Moreover, the visual color assessment and subject evaluation of textured fabrics will be adopted to demonstrate the effectiveness, and market feasibility of combining these two technologies to create various textures and patterns created on fabrics and appositeness to mass customization for consumer demands.

5.2 Limitations

One limitation of this research is the complexity of associated variables that can influence attributes of color, and all the variables weren't controlled in the experiment and reflected in the analysis part; thus, the result is not generalizable to other experiments. The color properties are not caused by a single independent factor, laser intensity.

Most of all, the scientific reliability and validity of the results can be improved with the additional samples and color measurements. The results should be obtained from replicated, triplicated, and reproducible sample developments.

In addition, in the case of inkjet printed pile surfaces, the total amount of reflected light is the sum of light reflected from the white sections as well as that from the colored tips. The proportion of the white section of colored fibers with height variation influences the appearance

of the material. Accordingly, studying the reflected light from the raw white cotton velvet fabric should have preceded to acquire the purely reflected light from the colored part of the fiber.

Furthermore, incident light could be transmitted, absorbed, scattered, reflected, and escaped on the fibers. With the same volume, finer fiber has a larger surface area than thicker fiber, and it increases the scattering of light and results in a lighter shade. Moreover, fibers with longer pile height can have lighter appearance due to the higher ratio of the uncolored white region of a fiber and increased scattering of light from larger surfaces. However, at the same time, the incident light can be trapped easily between the longer piles compared to shorter piles.

Besides, the chroma value obtained from the printed color can be inaccurate because the printed color is mixed as needed from combinations of distinct ink colors rather than an original pure ink. Accordingly, the chroma value of the printed color is often a complex combination of chroma values of mixed inks.

The colorfastness of the samples could be another factor that impacted the results. Improved colorfastness would benefit future research. Colorfastness and penetration of inkjet-printed dye can be improved through various attempts of adjusting pretreatment, ink formulation, drop size, and posttreatment conditions optimized for pile fabrics.

Pile lay orientation and flattened or bent pile, as well as wrinkles created throughout the whole process, may have contributed to the uneven color quality of samples and the results of instrumental color measurements. When a carpet loses its original appearance, shading and ridge effects often arise due to the variability in a pile lay orientation and pile compression (Pourdeyhimi et al., 1994).

Furthermore, ordinary inkjet printing systems impart small amounts of ink onto the piles, and the pile fibers require ink penetration (2018, March 12) to ensure satisfactory performance.

Like carpet, velvet pile can present similar challenges in inkjet printing and may require additional ink and larger drop size than that used for non-pile fabrics. Also, the accuracy of pile height measurement could be enhanced for future research.

REFERENCES

Abd El-Wahab, H., El-Molla, M. M., & Lin, L. (2010). Preparation and characterisation of ink formulations for jet printing on nylon carpet. *Pigment & Resin Technology, 39*(3), 163-169.

ASTM (1996). *E284. Standard terminology of appearance.* PA: American Society of Testing Materials.

Arthur, R. (2017). How digital printing technology is taking us closer to fully customizable clothing. *Forbes*, [Digital Image]. Retrieved from https://www.forbes.com/sites/rachelarthur/2017/02/17/digital-printing-technology-custom-clothing-fashion/#bb456266aef8

Ayau, M. R. (2018, September). There's something about textile. *Digital Printing Industry Insights*, (4), 8-10. Retrieved from http://www.flaar-reports.org/DPI/no4/mobile/index.html#p=10

Ayau, M. R. (2018, September). Reactive inks from fabric to output. *Digital Printing Industry Insights*, (4), 15-16. Retrieved from http://www.flaar-reports.org/DPI/no4/mobile/index.html#p=10

Bae, J. (2008). *Color in ink-jet printing: influence of structural and optical characteristics of textiles* (Doctoral dissertation, NC State University, Raleigh, United States). Retrieved from https://repository.lib.ncsu.edu/handle/1840.16/4425

Bae, J. H., Hong, K. H., & Lamar, T. M. (2015). Effect of texture on color variation in inkjet-printed woven textiles. *Color Research & Application, 40*(3), 297-303.

Bahtiyari, M. I. (2011). Laser modification of polyamide fabrics. *Optics & Laser Technology, 43*(1), 114-118.

Baumann, W., Kleinemeier, N., Brossman, R., Oesch, H. P., Krayer, M., Groebel, B. T., & Leaver, A. T. (1987). Determination of relative colour strength and residual colour difference by means of reflectance measurements. *Journal of the Society of Dyers and Colourists, 103*, 100-5.

Belli, R., Miotello, A., Mosaner, P., & Toniutti, L. (2005). Laser cleaning of ancient textiles. *Applied surface science, 247*(1-4), 369-372.

Berns, R. S. (2000). *Billmeyer and Saltzman's principles of color technology*. NY: Wiley.

Berns, R. S. (2019). *Billmeyer and Saltzman's principles of color technology*. John Wiley & Sons.

Bogue, R. (2015). Lasers in manufacturing: a review of technologies and applications. *Assembly Automation, 35*(2), 161-165.

Brandon, K. (2008, July). The luxury, the indulgence that is velvet. *FIBRE2FASHION.COM*, Retrieved from https://www.fibre2fashion.com/industry-article/3471/the-luxury-the-indulgence-that-is-velvet-

Bordeaux Digital PrintInk Ltd. (n.d.). Bordeaux's revolutionary latex ink for textiles: one ink for all fabrics. *Bordeaux Digital Printink*, Retrieved from https://www.c-m-y-k.com/bordeauxs-revolutionary-latex-ink-for-textiles-one-ink-for-all-fabrics/

Campbell, J. R. (2006). Controlling digital colour printing on textiles. In H. Xin (Eds.), *Total Colour Management in Textiles* (pp. 160-190). Cambridge: Woodhead Publishing.

Carr, W. W., Park, H., Ok, H., Furbank, R., Dong, H., & Morris, J. F. (2006). Drop formation and impaction. *Digital printing of textiles, 2*(1), 53-68.

ElEn Industrial Laser Division. (n.d.). Laser engraving leather: an asset for the fashion and decorating industry. [Digital Image]. Retrieved from https://elenlaser.com/blog/laser-

engraving-leather-asset-fashion-decorating-industry.html

Chapman, L. P., & Istook, C. L. (2002). Virtual designing in 3D for textile printing. In *NIP & Digital Fabrication Conference* (pp. 249-253). VA: Society for Imaging Science and Technology.

Chen, W., Wang, G., & Bai, Y. (2002). Best for wool fabric printing–digital inkjet. *Textile Asia, 33*(12), 37-39.

Choudhary, K. (2018). Engineered digital textile print design for customized curves. *Journal of Textile and Apparel, Technology and Management, 10*(3). 1-9.

Choudhury, A. K. R. (2014a). *Principles of colour and appearance measurement: Object appearance, colour perception and instrumental measurement*. NY: Elsevier.

Choudhury, A. K. R. (2014b). *Principles of colour and appearance measurement: Visual measurement of colour, colour comparison and management*. NY: Elsevier.

Cie, C. (2015). *Inkjet textile printing*. NY: Elsevier.

Conover, W. J., & Conover, W. J. (1999). *Practical nonparametric statistics.* NY: John Wiley & Sons.

Datacolor. (n.d.). Datacolor match textile. [Digital Image]. Retrieved from https://www.datacolor.com/business-solutions/product-overview/datacolor-match-textile/

Daplyn, S., & Lin, L. (2003). Evaluation of pigmented ink formulations for jet printing onto textile fabrics. *Pigment & resin technology, 32*(5), 307-318.

Ding, Y., Shamey, R., Chapman, L. P., & Freeman, H. S. (2019). Pretreatment effects on pigment-based textile inkjet printing–colour gamut and crockfastness properties. *Coloration Technology, 135*(1), 77-86.

Dorsey, J., Rushmeier, H., & Sillion, F. (2010). *Digital modeling of material appearance*. NY: Elsevier.

Dowden, J. (2009). Laser keyhole welding: the vapour phase. In *The Theory of Laser Materials Processing* (pp. 95-128). Springer, Dordrecht.

Durmus, D. (2018). *Optimising light source spectrum to reduce the energy absorbed by objects* (Doctoral dissertation, The University of Sydney, Australia). [Digital Image]. Retrieved from https://ses.library.usyd.edu.au/handle/2123/17844

Dwivedi, A. K., Mallawaarachchi, I., & Alvarado, L. A. (2017). Analysis of small sample size studies using nonparametric bootstrap test with pooled resampling method. *Statistics in medicine, 36*(14), 2187-2205.

Endo, M., Kitaguchi, S., Morita, H., Sato, T., & Sukigara, S. (2013). Characterization of fabrics using the light reflectance and the surface geometry measurements. *Journal of Textile Engineering, 59*(4), 75-81.

Fan, Q., Kim, Y. K., Lewis, A. F., & Perruzzi, M. K. (2002, January). Effects of pretreatments on print qualities of digital textile printing. In *NIP & Digital Fabrication Conference* (Vol. 2002, No. 1, pp. 236-241). Society for Imaging Science and Technology.

Fan, Q., Kim, Y. K., Perruzzi, M. K., & Lewis, A. F. (2003). Fabric pretreatment and digital textile print quality. *Journal of Imaging Science and Technology, 47*(5), 400-407.

Fan, Q., Xue, H., & Kim, Y. K. (2008). Effect of UV curable pretreatments on the color quality of inkjet printed polyester fabrics. *Research Journal of Textile and Apparel, 12*(1), 1-8.

Friedman, M. (1940). A comparison of alternative tests of significance for the problem of m rankings. *The Annals of Mathematical Statistics, 11*(1), 86-92.

Gladstone, M. J. (1970). *A pile fabric primer: corduroy/velveteen/velvet*. NY: M.J. Crompton-Richmond Company.

Gong, R. H. (2015). Yarn to fabric: specialist fabric structures. In R. Sinclair (Eds.), *Textiles and Fashion: Materials, Design and Technology* (pp. 337-354). Cambridge: Woodhead Publishing.

Gorji Kandi, S., Amani Tehran, M., & Rahmati, M. (2008). Colour dependency of textile samples on the surface texture. *Coloration Technology, 124*(6), 348-354.

Hawkyard, C. (2006). Substrate preparation for ink-jet printing. In H. Ujiie (Eds.), *Digital Printing of Textiles* (pp. 201-217). Cambridge: Woodhead Publishing,

Horrocks, A. R., & Anand, S. C. (Eds.). (2000). *Handbook of technical textiles*. NY: Elsevier.

EpilogLaser. (n.d.). How to laser engrave a child's fleece jacket. [Digital Image]. Retrieved from https://www.epiloglaser.com/resources/sample-club/fleece-jacket.htm

Hermeymonica. (n.d.). The cross section of velvet fabric [Digital image]. Retrieved from: https://www.google.com/imgres?imgurl=http://www.hermeymonica.com/upload/2019/01/04/fancy-weaves-axeminster-carpet-l-2b588b98bea7e118.jpg&imgrefurl=http://www.hermeymonica.com/axeminster-carpet/&h=546&w=728&tbnid=y7Y2LmqScZLnmM&tbnh=194&tbnw=259&usg=AI4_-kRkri2QQ2BLsRsgumLwd9dZ4UBr2A&vet=1&docid=LfsxaFgVSO0NaM

Hider, C. E. (2018). *Assessment of digital inkjet printing on jacquard woven base cloths* (Master's thesis, NC State University, Raleigh, United States). Retrieved from http://www.lib.ncsu.edu/resolver/1840.20/35170

HP. (2011 October). HP latex printing technologies 2012 [PDF file]. Retrieved from http://www.hp.com/hpinfo/newsroom/press_kits/2011/HPLatexSummit/LatexTechnology

.pdf

HP. (2012 May). The HP latex printing solution for temporary textiles [PDF file]. Retrieved from http://media.flixcar.com/media/inpage/assetsv2/HP-25763582-4AA3-9727ENW.pdf

Hunt, R. W. G. (2005). *The reproduction of colour*. NY: John Wiley & Sons.

Hunt, R. W. G., & Pointer, M. R. (2011). *Measuring colour*. NY: John Wiley & Sons.

HunterLab. (2008). The Kubelka-Monk theory and K/S [PDF file]. Retrieved from https://www.hunterlab.se/wp-content/uploads/2012/11/The-Kubelka-Monk-Theory-and-K-S.pdf

Latex vs solvent. (March 04, 2014). *Image Reports*. Retrieved from https://www.imagereportsmag.co.uk/features/technical/tech-knowledge/4716-latex-vs-solvent

Janssen, B. G. G. (2017). *Print quality of digital inkjet printed nonwoven fabrics* (Doctoral dissertation, NC State University, Raleigh, United States). Retrieved from https://repository.lib.ncsu.edu/handle/1840.20/34435

Johnsen, S. (2016). How to measure color using spectrometers and calibrated photographs. *Journal of Experimental Biology, 219*(6), 772-778.

Jordan, D. M. (2001). Color tolerances in textile manufacture. *AATCC review, 1*(9), 76-80.

Judd, D. B., Wyszecki, G., & Wintringham, W. T. (1963). Color in business, science, and industry. *Physics Today*, *16*, 74.

Kan, C. W. (2014). Colour fading effect of indigo-dyed cotton denim fabric by CO2 laser. *Fibers and Polymers, 15*(2), 426-429.

Kan, C. W., & Yuen, C. W. M. (2012). Digital ink-jet printing on textiles. *Research Journal of Textile and Apparel, 16*(2), 1-24.

Kan, C. W., Yuen, C. W. M., & Cheng, C. W. (2010). Technical study of the effect of CO2 laser surface engraving on the colour properties of denim fabric. *Coloration Technology, 126*(6), 365-371.

Kan, C. W., Yuen, C. W. M., & Tsoi, W. Y. (2011). Using atmospheric pressure plasma for enhancing the deposition of printing paste on cotton fabric for digital ink-jet printing. *Cellulose, 18*(3), 827-839.

Kang, H. R. (2006). *Computational color technology*. Bellingham: Spie Press.

Kapfunde, M. (2017). The denim industry, at the intersection of people, planet and purpose. *FashNerd*, [Digital Image]. Retrieved from https://fashnerd.com/2017/09/sustainable-denim-technology-bleuezone/

King, K. M. (2013). Inkjet printing of technical textiles. In M.L. Gulrajani (Eds.), *Advances in the Dyeing and Finishing of Technical Textiles* (pp. 236-257). Cambridge: Woodhead Publishing.

Kitaguchi, S., Westland, S., & Luo, M. R. (2005). Suitability of texture analysis methods for perceptual texture. *Proceedings, 10th Congress of the International Colour Association, 10*, 923-926.

Lee, P. (2018, September). Textile inkjet inks for digital printers. *Digital Printing Industry Insights*, (4), 12-13. Retrieved from: http://www.flaar-reports.org/DPI/no4/mobile/index.html#p=10.

Leelajariyakul, S., Noguchi, H., & Kiatkamjornwong, S. (2008). Surface modified and micro-encapsulated pigmented inks for ink jet printing on textile fabrics. *Progress in Organic Coatings, 62*(2), 145-161.

Lim, J., & Chapman, L. P. (2019). Fabric surface characteristics and their impact on digital

textile printing quality of PET fabrics. *AATCC Journal of Research, 6*(1), 1-9.

Liu, Z., Fang, K., Gao, H., Liu, X., & Zhang, J. (2016). Effect of cotton fabric pretreatment on drop spreading and colour performance of reactive dye inks. *Coloration Technology, 132*(5), 407-413.

Luo, M. R. (2006). Colour quality evaluation. In J Xin (Eds.), *Total Colour Management in Textiles* (pp. 57-75). Cambridge: Woodhead Publishing.

Luo, L., Tsang, K. M., Shen, H. L., Shao, S. J., & Xin, J. H. (2015). An investigation of how the texture surface of a fabric influences its instrumental color. *Color Research & Application, 40*(5), 472-482.

McDonald, R. (Ed.). (1997). *Colour physics for industry* (2nd ed.). Bradford: Society of Dyers and Colourists.

Mhetre, S., Carr, W., & Radhakrishnaiah, P. (2010). On the relationship between ink-jet printing quality of pigment ink and the spreading behavior of ink drops. *The Journal of the Textile Institute, 101*(5), 423-430.

ValueJet 1938TX (n.d.). *MUTOH*. Retrieved from http://www.mutoh.eu/en-us/products/directtextile/valuejet1938tx.aspx#27638106-specifications

National Institute of Standards and Technology. (2015). Friedman test. Retrieved from https://www.itl.nist.gov/div898/software/dataplot/refman1/auxillar/friedman.htm

Nayak, R., & Padhye, R. (2016). The use of laser in garment manufacturing: an overview. *Fashion and textiles, 3*(1), 5.

Ohno, Y. (2000, January). CIE fundamentals for color measurements. In *NIP & Digital Fabrication Conference* (Vol. 2000, No. 2, pp. 540-545). Society for Imaging Science and Technology.

Ondogan, Z., Pamuk, O., Ondogan, E. N., & Ozguney, A. (2005). Improving the appearance of all textile products from clothing to home textile using laser technology. *Optics & Laser Technology, 37*(8), 631-637.

Park, H., Carr, W. W., Ok, H., & Park, S. (2006). Image quality of inkjet printing on polyester fabrics. *Textile research journal, 76*(9), 720-728.

Pourdeyhimi, B. (1994). Evaluating carpet appearance loss: Color change. *Textile research journal, 64*(8), 485-490.

Pourdeyhimi, B., Xu, B., & Nayernouri, A. (1994). Evaluating carpet appearance loss: pile lay orientation. *Textile Research Journal, 64*(3), 130-135.

Raymond, M. (2006). Industrial production printers–DuPont Artistri™ 2020 textile printing system. In H. Ujiie (Eds.), *Digital printing of textiles* (pp. 69-83). Cambridge: Woodhead Publishing.

Redmore, N. A. (2011). Woven textile design. In A. Briggs-Goode and K. Townsend (Eds.), *Textile Design* (pp. 31-54). Cambridge: Woodhead Publishing.

Renzo, S. (2018). TC707: Color science laboratory manual [Course Resource]. NC State University. Polymer and Color Chemistry Program.

Shahidi, S., Moazzenchi, B., & Ghoranneviss, M. (2013). Improving the dyeability of polypropylene fabrics using laser technology. *Journal of The Textile Institute, 104*(10), 1113- 1117.

Shao, S. J., Xin, J. H., Zhang, Y., & Li, M. Z. (2006). The effect of texture structure on instrumental and visual color difference evaluation. *AATCC review, 6*(10), 42-48.

Pericot, J.R. (2016 September 28). Understanding latex technology. *SIGN & Digital Graphics*. Retrieved from https://sdgmag.com/features/understanding-latex-technology

The Minitab Blog Editor. (2015). Repeated measures designs: Benefits, challenges, and an ANOVA example. *The Minitab Blog*. Retrieved from https://blog.minitab.com/blog/adventures-in-statistics-2/repeated-measures-designs-benefits-challenges-and-an-anova-example

Tyler, D.J. (2005). Textile digital printing technologies. *Textile Progress, 37*, 1-65.

Universal Laser Systems. (2017 March). VLS Platform Series. Retrieved from https://cdn.ulsinc.com/assets/pdf/platforms/592b989776b6741c15762265/vls_platform_spec_sheet__2017-03.pdf

Universal Laser Systems. (2010). VersaLASER® (VLS) user guide VLS3.60, VLS4.60, VLS6.60. Retrieved from https://peoplevine.blob.core.windows.net/media/397/business/3598/VLS_Platform_User_Guide.pdf

Venkatraman, P. D., & Liauw, C. M. (2019). Use of a carbon dioxide laser for environmentally beneficial generation of distressed/faded effects on indigo dyed denim fabric: Evaluation of colour change, fibre morphology, degradation and textile properties. *Optics & Laser Technology*, *111*, 701-713.

Vilumsone-Nemes, I. (2018). *Industrial cutting of textile materials*. Cambridge: Woodhead Publishing.

Wakayama. (2017). Shima presents its digital textile printing offering [Digital Image]. Retrieved from https://www.knittingindustry.com/shima-presents-its-digital-textile-printing-offering/

Wastradowski, M. (n.d.). Thermal printers vs. inkjet printers [Digital Image]. *Graphic Products*. Retrieved from https://www.graphicproducts.com/articles/thermal-printers-vs-inkjet-

printers/

Westland, S., & Cheung, V. (2006). Colour perception. In H. Xin (Eds.), *Total Colour Management in Textiles* (pp. 7-21). Cambridge: Woodhead Publishing.

Williams-Alvarez, J. (2014 June 17). What you need to know about laser-cut clothing [Digital Image]. *Engadget*. Retrieved from https://www.engadget.com/2014/06/17/laser-cut-clothing-explainer/

Wood, E. J. (1993). Description and measurement of carpet appearance. *Textile research journal, 63*(10), 580-594.

Xin, J. H., Shen, H. L., & Chuen Lam, C. (2005). Investigation of texture effect on visual colour difference evaluation. *Color Research and Application, 30*(5), 341-347.

X-Rite. (2019). DE2000 vs. DEcmc. Retrieved from https://www.xrite.com/service-support/de2000vsdecmc

Yang, Y., & Li, S. (2003). Cotton fabric inkjet printing with acid dyes. *Textile research journal, 73*(9), 809-814.

YPS. (n.d.). HP latex 115 printer [Digital Image]. Retrieved from: https://www.yourprintspecialists.co.uk/product/hp-latex-115-printer-2/

Yuan, G., Jiang, S., Newton, E., Fan, J., & Au, W. (2012). Embellishment of fashion design via laser engraving. *Research Journal of Textile and Apparel, 16*(4), 106-111.